Lattice Effective Field Theory Simulations of Nuclei

Dean Lee
Facility for Rare Isotope Beams
Michigan State University
Nuclear Lattice EFT Collaboration

Light-Ion Physics with EIC
Wednesday, March 4, 2026

Outline

Nuclear lattice effective field theory

Pinhole algorithm

Clustering in light nuclei

Wavefunction matching

Charge radii of silicon isotopes

Structure of beryllium isotopes

Superfluid condensation

Multimodal superfluidity of neutrons

Summary

Nuclear lattice effective field theory

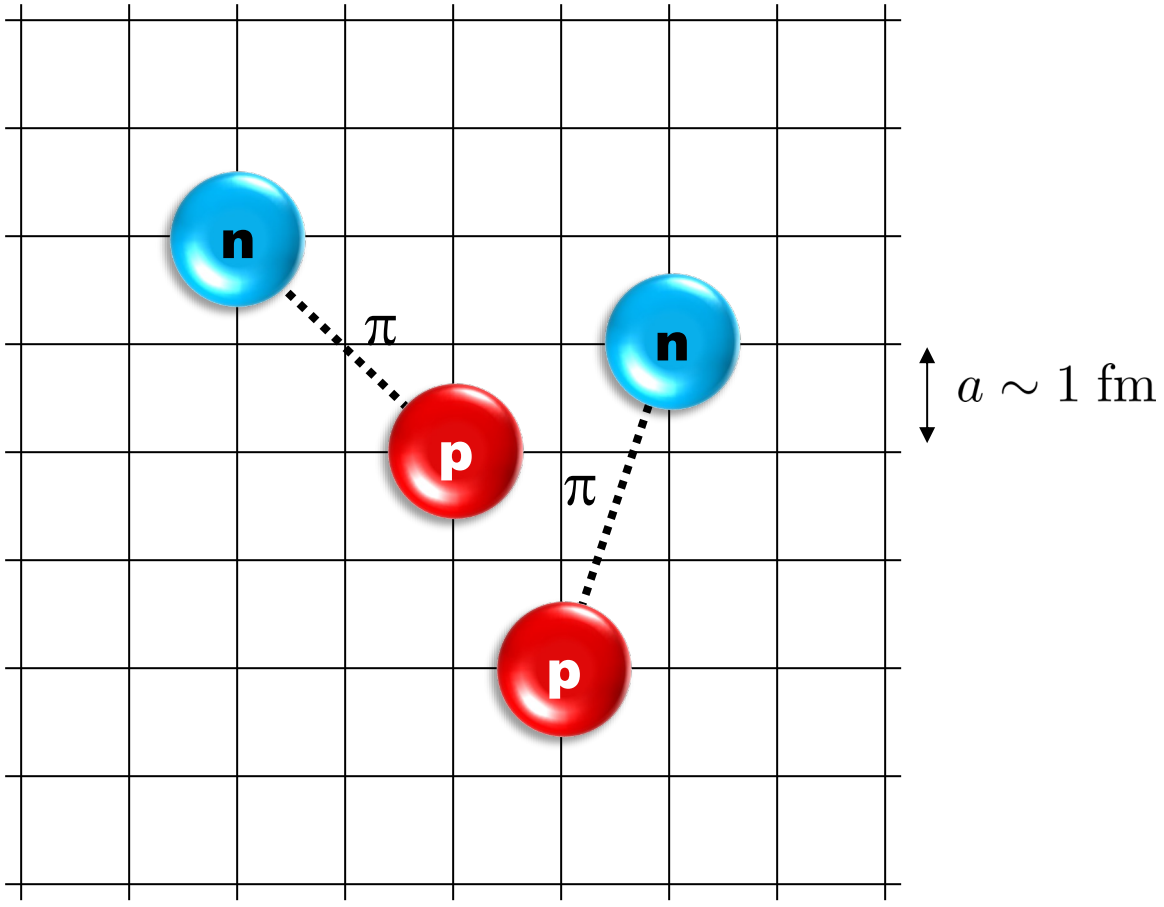

D.L, Prog. Part. Nucl. Phys. 63 117-154 (2009); D.L., arXiv:2501.03303

Lähde, Meißner, Nuclear Lattice Effective Field Theory (2019), Springer

Chiral effective field theory

Construct the effective potential order by order

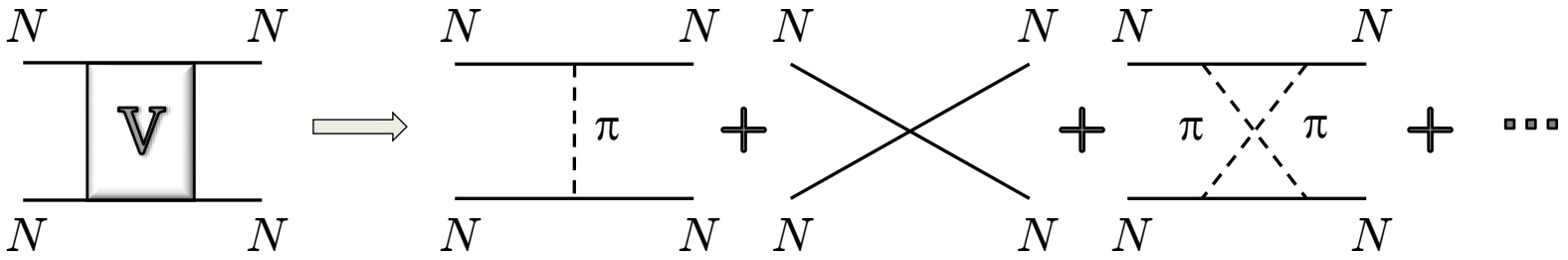

$a = 1.315\,\mathrm{fm}$

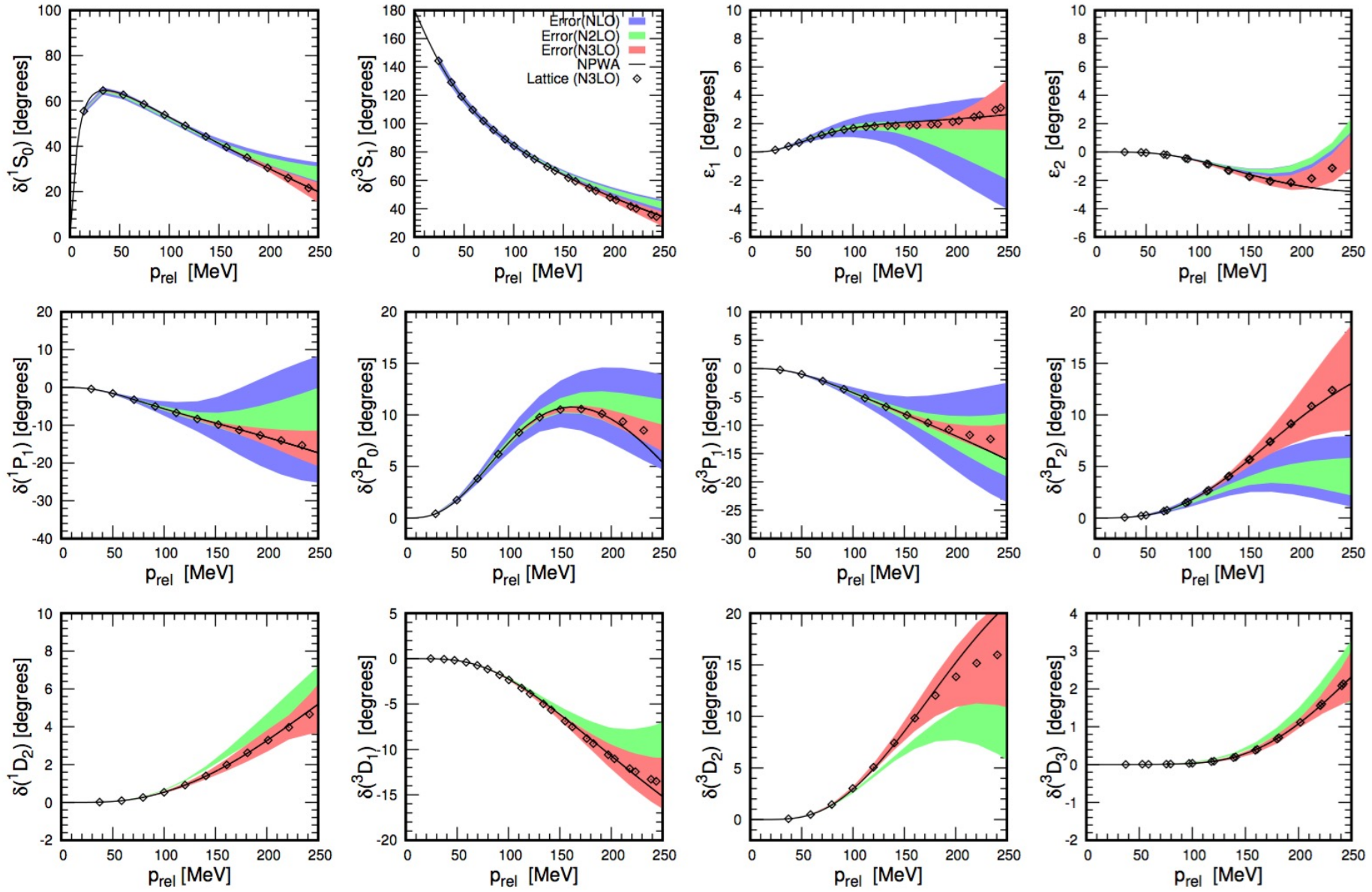

Li, Elhatisari, Epelbaum, D.L., Lu, Meißner, PRC 98, 044002 (2018)

$a = 0.987\,\mathrm{fm}$

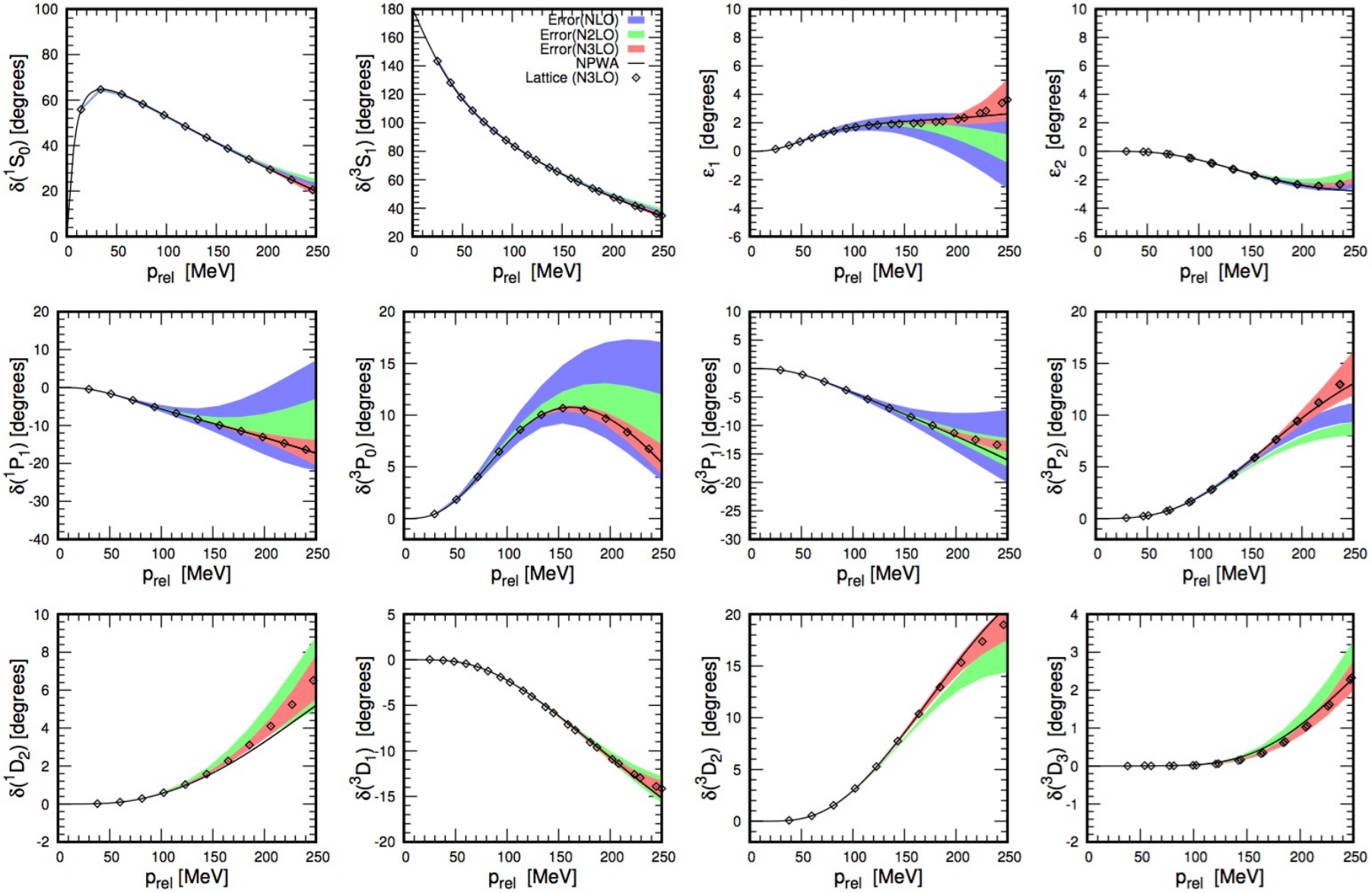

Euclidean time projection

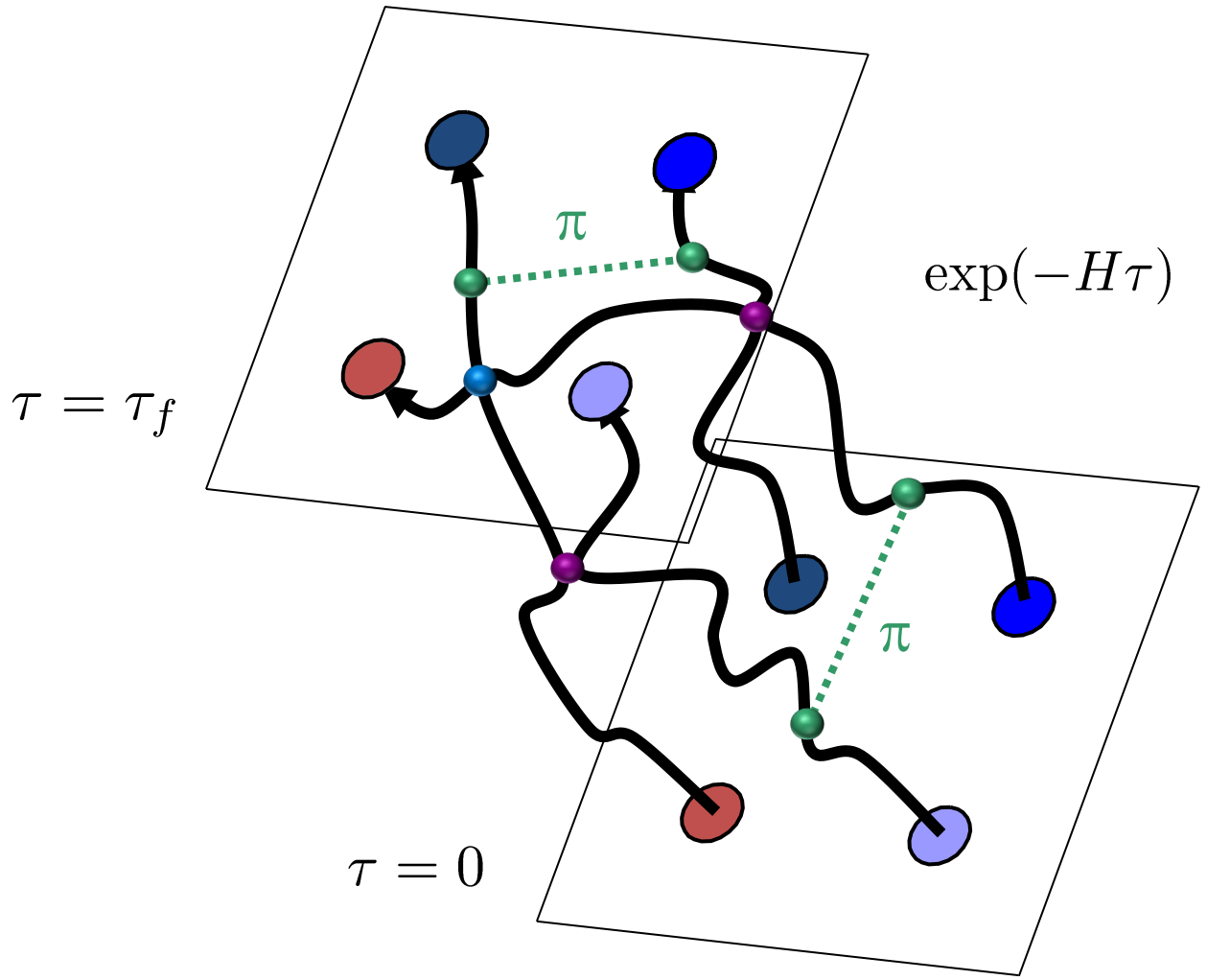

Auxiliary field method

We can write exponentials of the interaction using a Gaussian integral identity

$$\exp\left[-\frac{C}{2}(N^\dagger N)^2\right] \qquad \times \quad (N^\dagger N)^2$$

$$= \sqrt{\frac{1}{2\pi}} \int_{-\infty}^{\infty} ds \exp\left[-\frac{1}{2}s^2 + \sqrt{-C}\, s(N^\dagger N)\right] \qquad \rangle \bullet \quad sN^\dagger N$$

We remove the interaction between nucleons and replace it with the interactions of each nucleon with a background field.

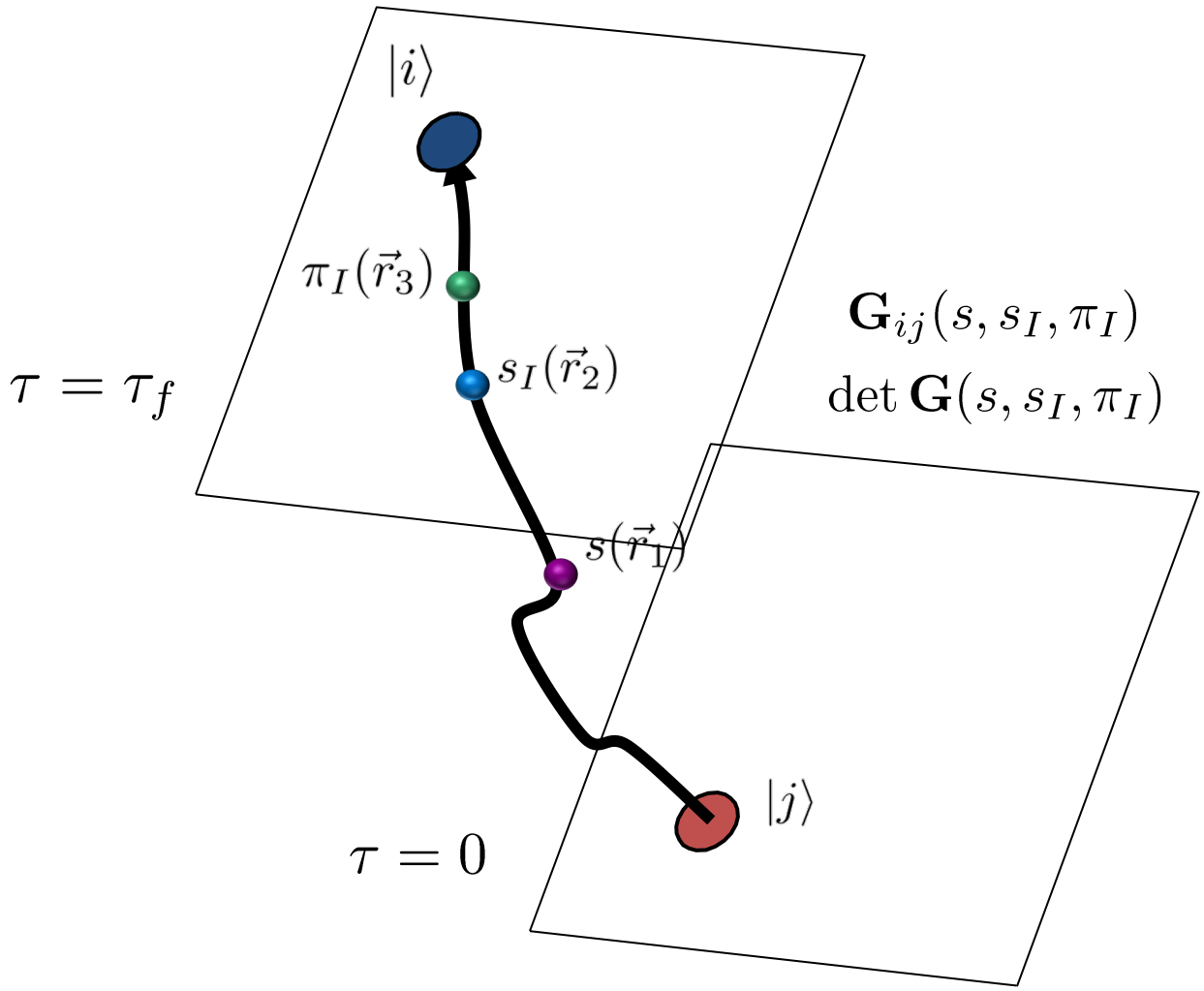
$|i\rangle$
$\pi_I(\vec{r}_3)$
$s_I(\vec{r}_2)$
$s(\vec{r}_1)$
$|j\rangle$
$\tau = \tau_f$
$\tau = 0$
$\mathbf{G}_{ij}(s, s_I, \pi_I)$
$\det \mathbf{G}(s, s_I, \pi_I)$

Essential elements for nuclear binding

$$H = H_{\rm free} + \tfrac{1}{2!} C_2 \sum_{\mathbf{n}} \tilde{\rho}(\mathbf{n})^2 + \tfrac{1}{3!} C_3 \sum_{\mathbf{n}} \tilde{\rho}(\mathbf{n})^3 + V_{\rm Coulomb}$$

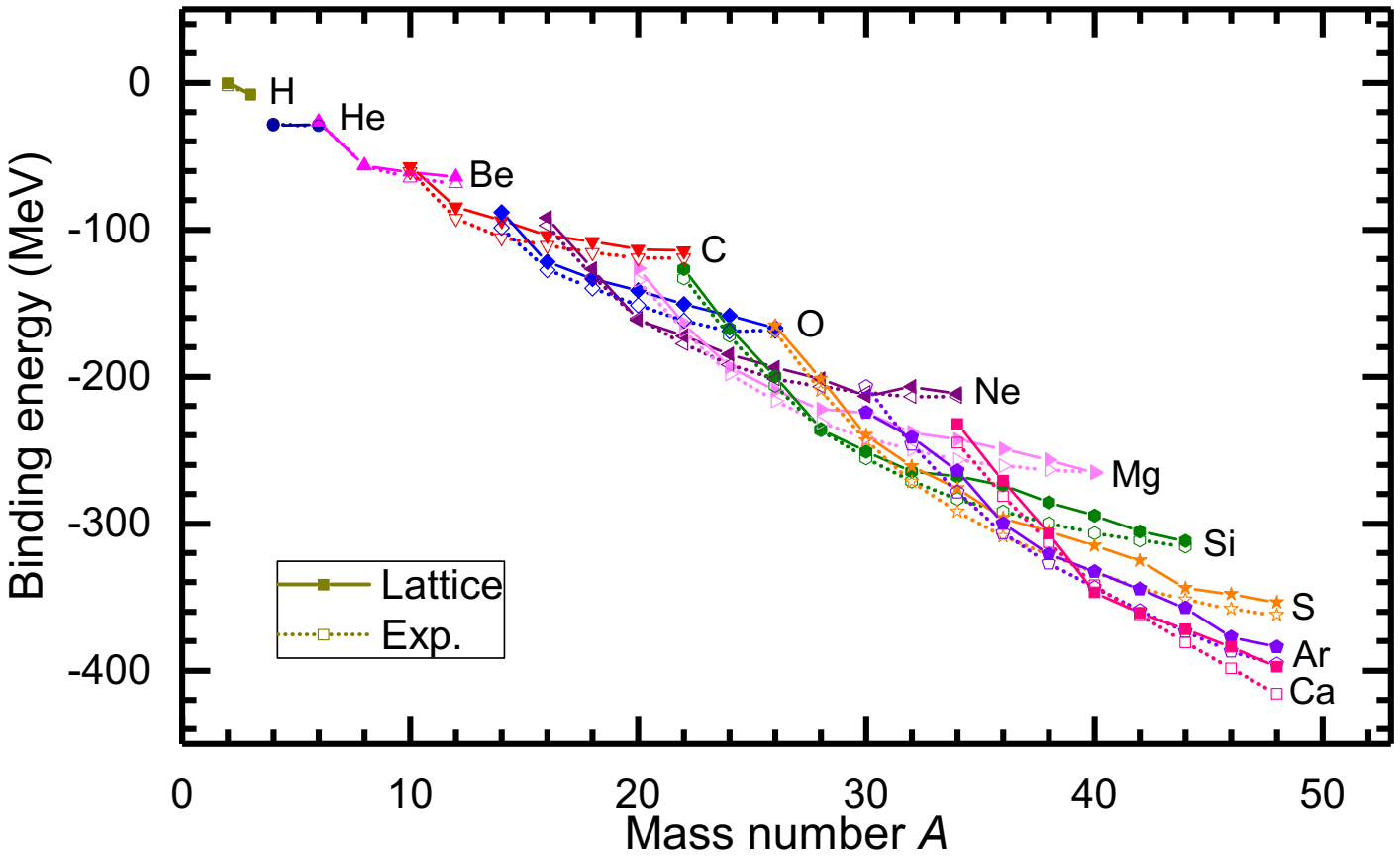

Lu, Li, Elhatisari, D.L., Epelbaum, Meißner, PLB 797, 134863 (2019)

Pinhole algorithm

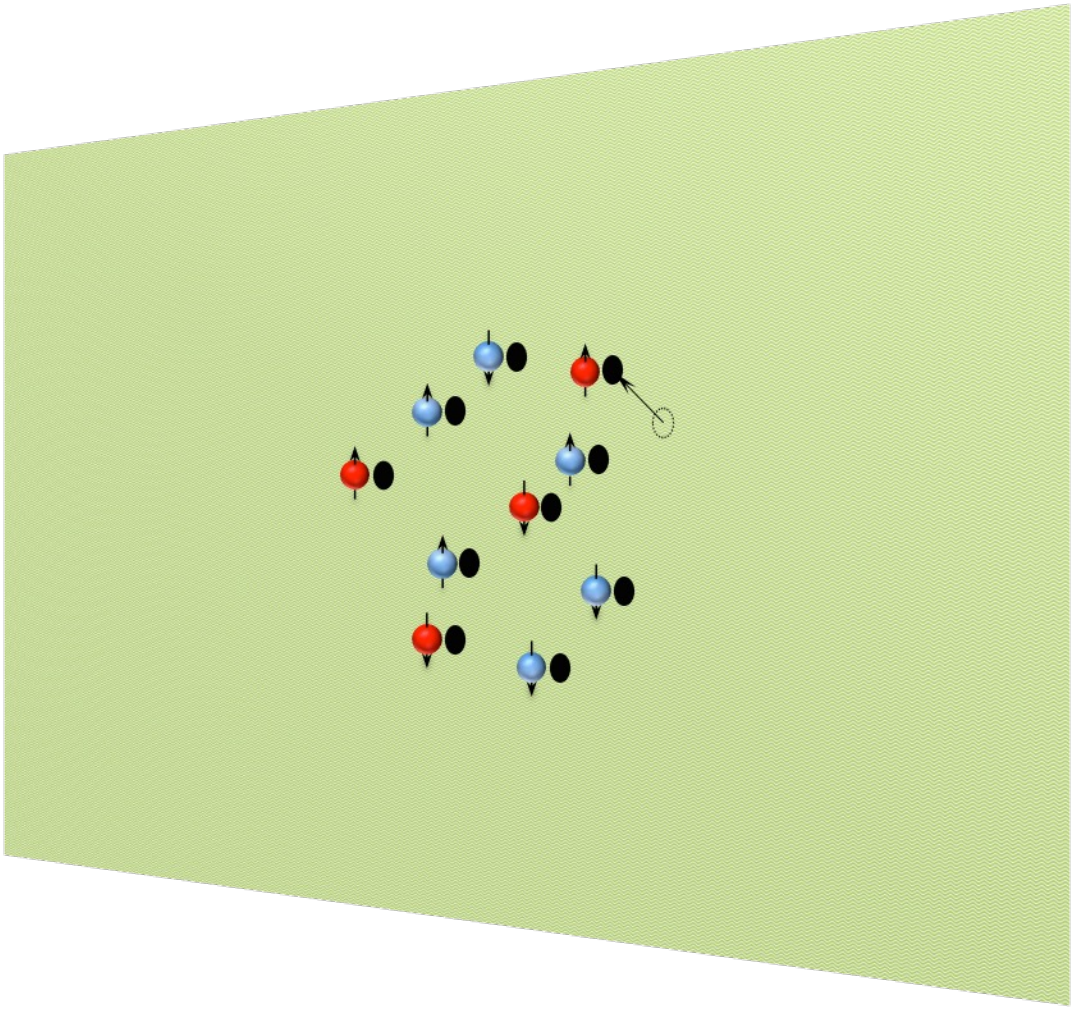

Elhatisari, Epelbaum, Krebs, Lähde, D.L., Li, Lu, Meißner, Rupak, PRL 119, 222505 (2017)

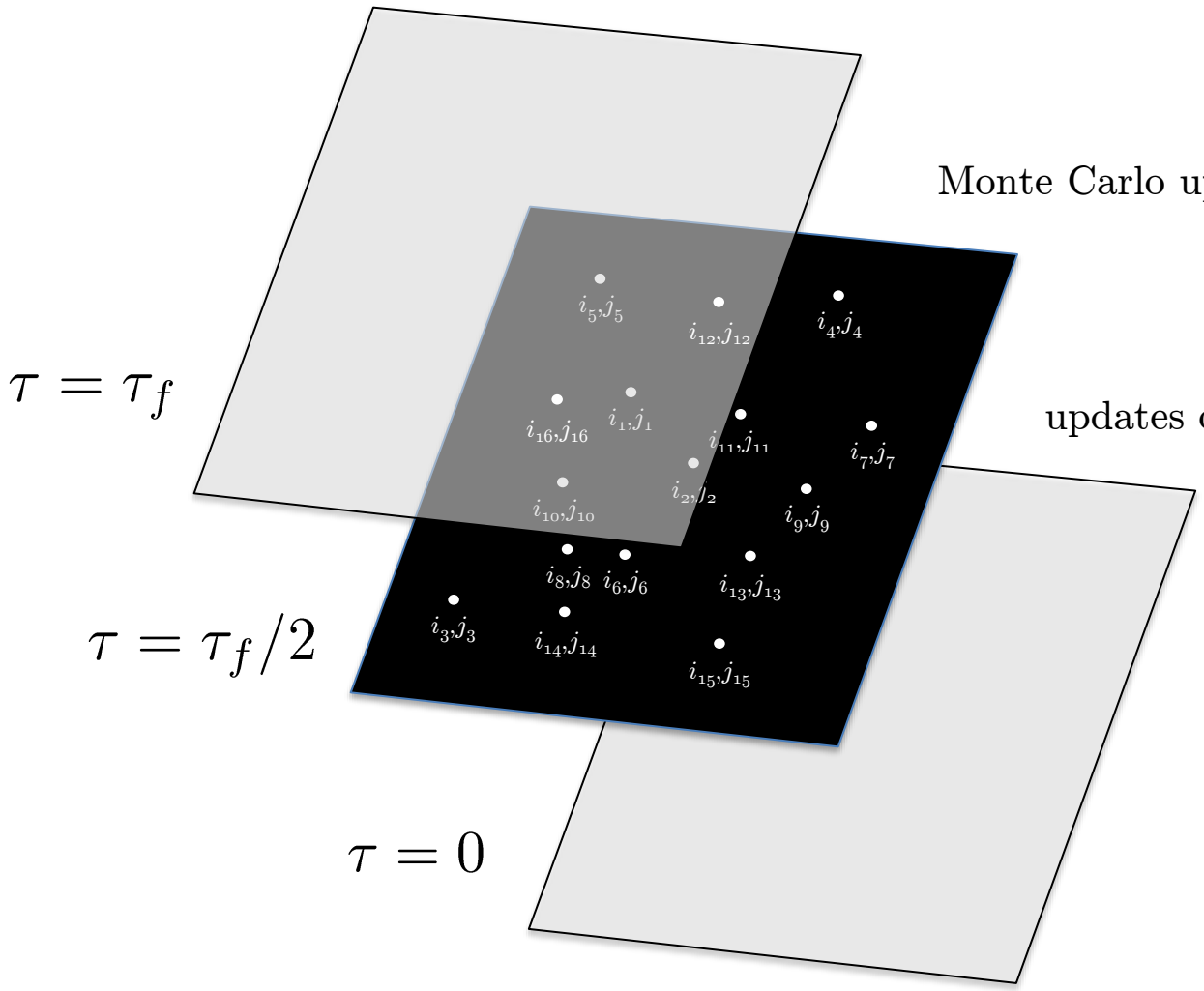

Monte Carlo updates of pinholes

Monte Carlo
updates of auxiliary/pion fields

Elhatisari, Epelbaum, Krebs, Lähde, D.L., Li, Lu, Meißner, Rupak, PRL 119, 222505 (2017)

^{16}O

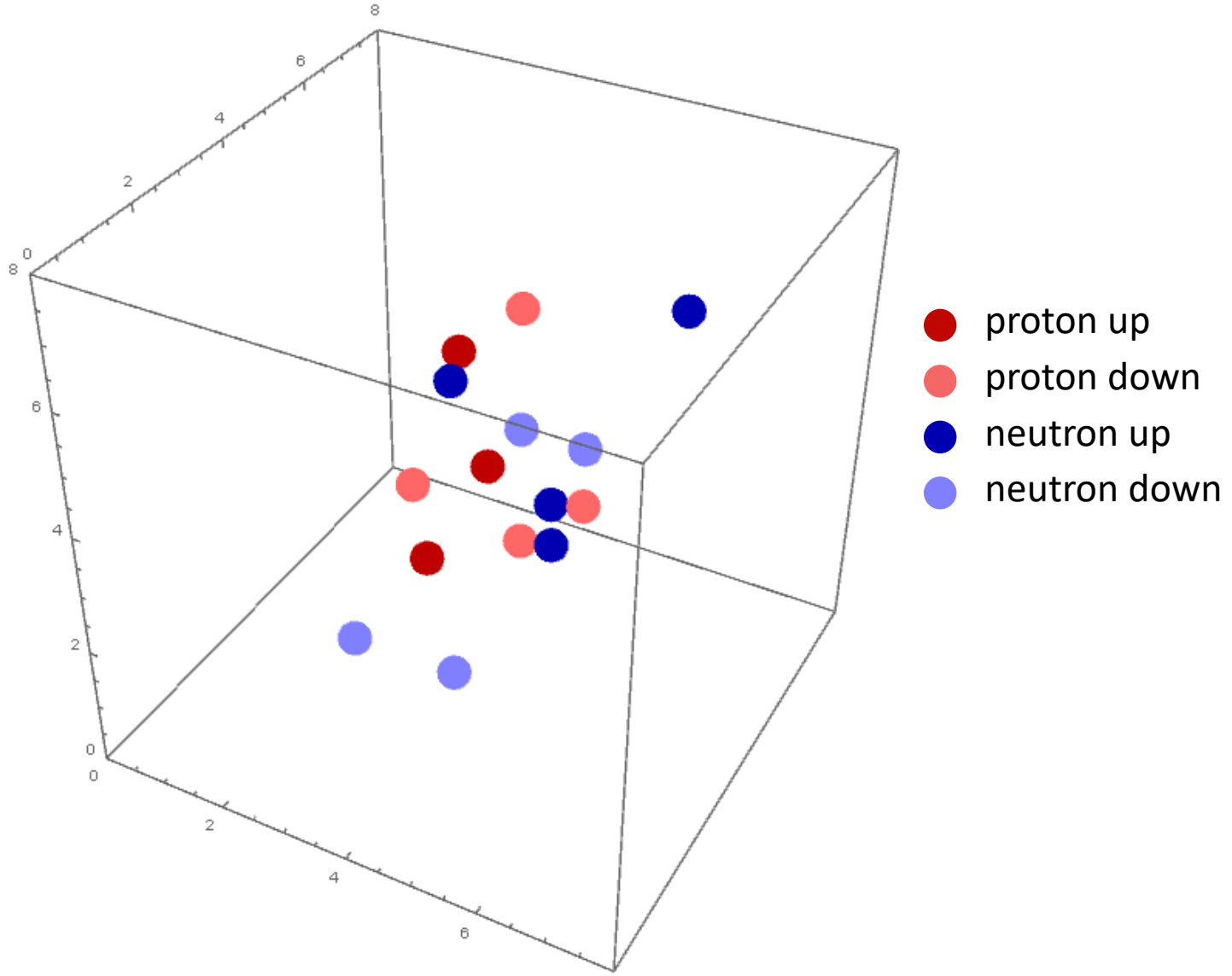

Summerfield, Lu, Plumberg, D.L., Noronha-Hostler, Timmins, Phys. Rev. C 104 L041901 (2021)

Structure of ^{16}O and ^{20}Ne

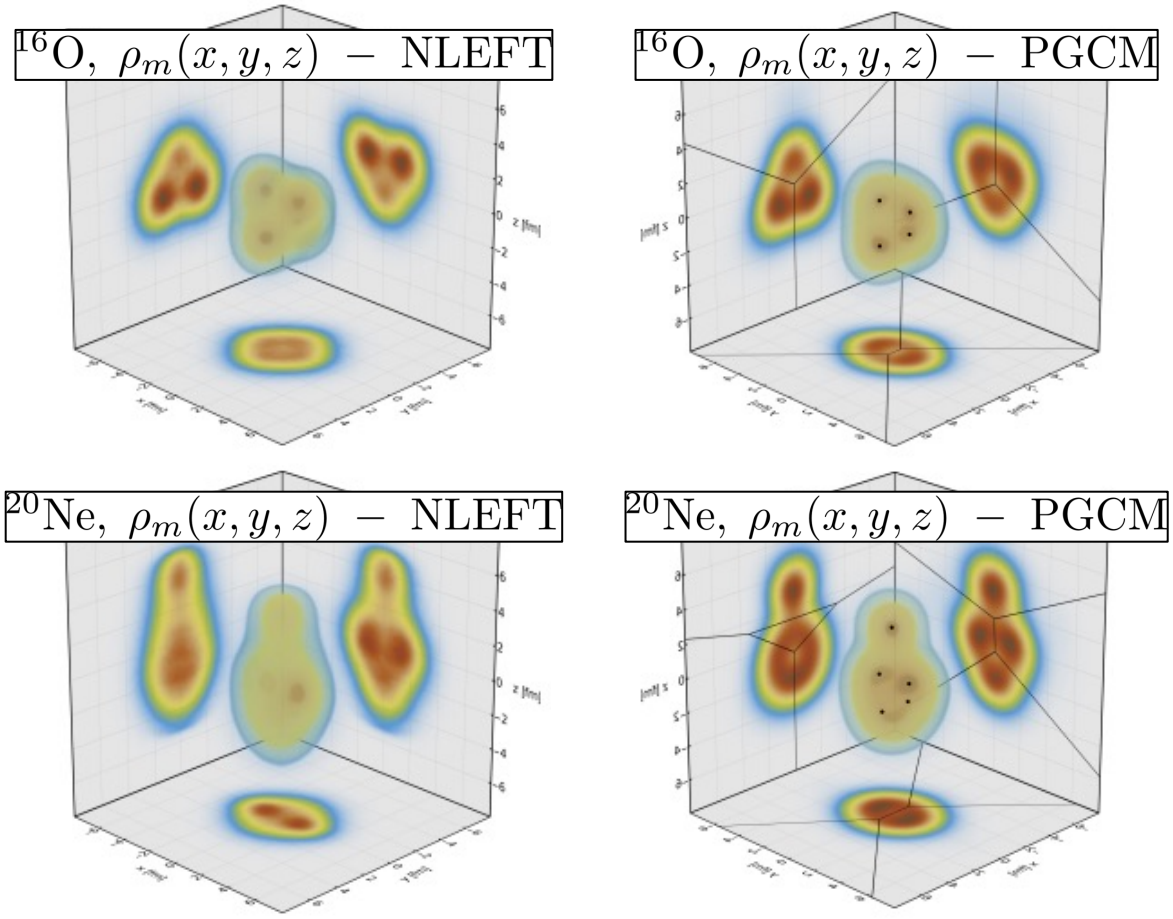

Giacalone et al., Phys. Rev. Lett. 135, 012302 (2025)

Giacalone et al., Phys. Rev. Lett. 134, 082301 (2025)

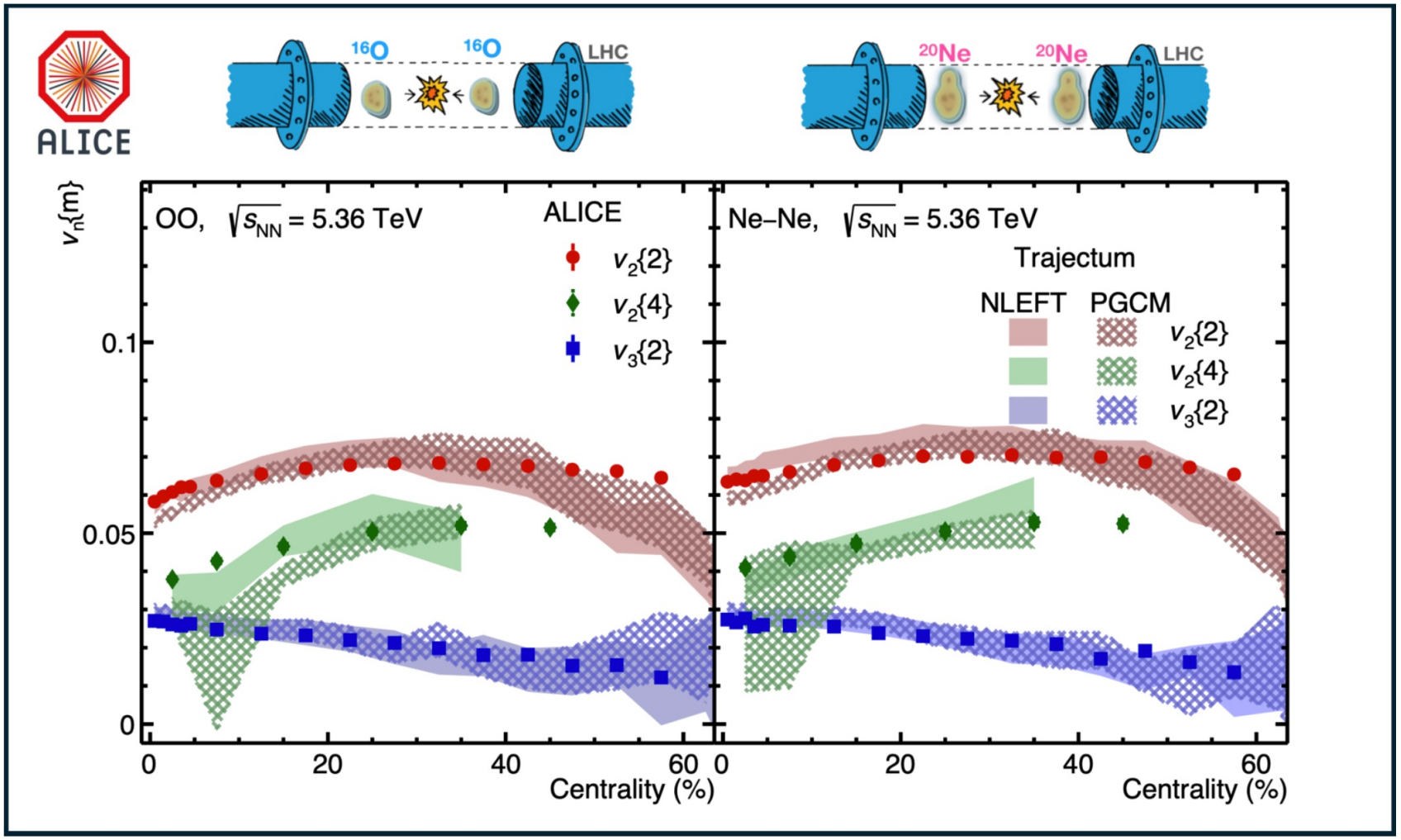

ALICE Collab., "Evidence of nuclear geometry-driven anisotropic flow in OO and Ne–Ne collisions at $\sqrt{s_{NN}}$ = 5.36 TeV", https://arxiv.org/abs/2509.06428

Emergent geometry and duality of ^{12}C

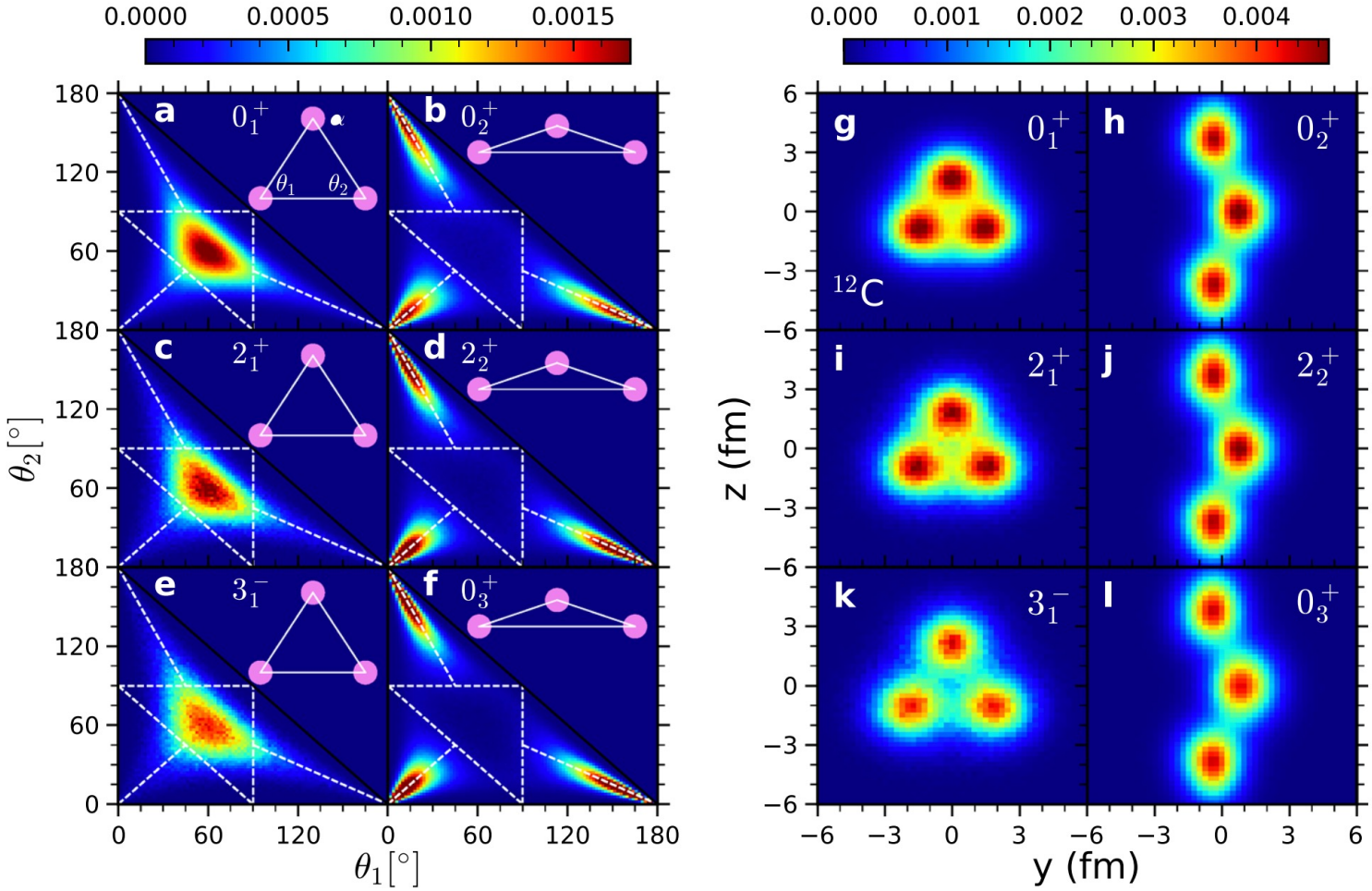

Shen, Elhatisari, Lähde, D.L., Lu, Meißner, Nature Commun. 14, 2777 (2023)

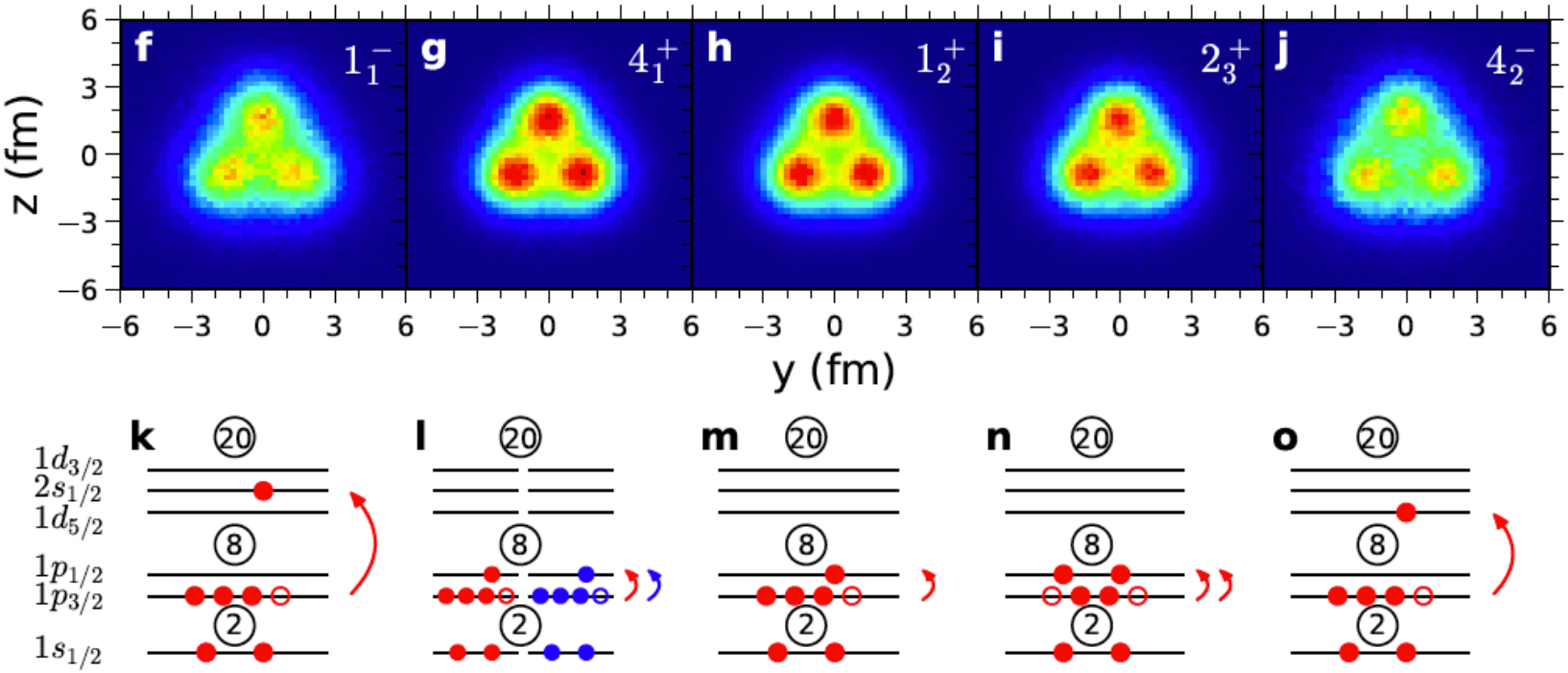
f
1^-_1
g
4^+_1
h
1^+_2
i
2^+_3
j
4^-_2
z (fm)
y (fm)
6
3
0
−3
−6
k
l
m
n
o
20
8
2
$1d_{3/2}$
$2s_{1/2}$
$1d_{5/2}$
$1p_{1/2}$
$1p_{3/2}$
$1s_{1/2}$

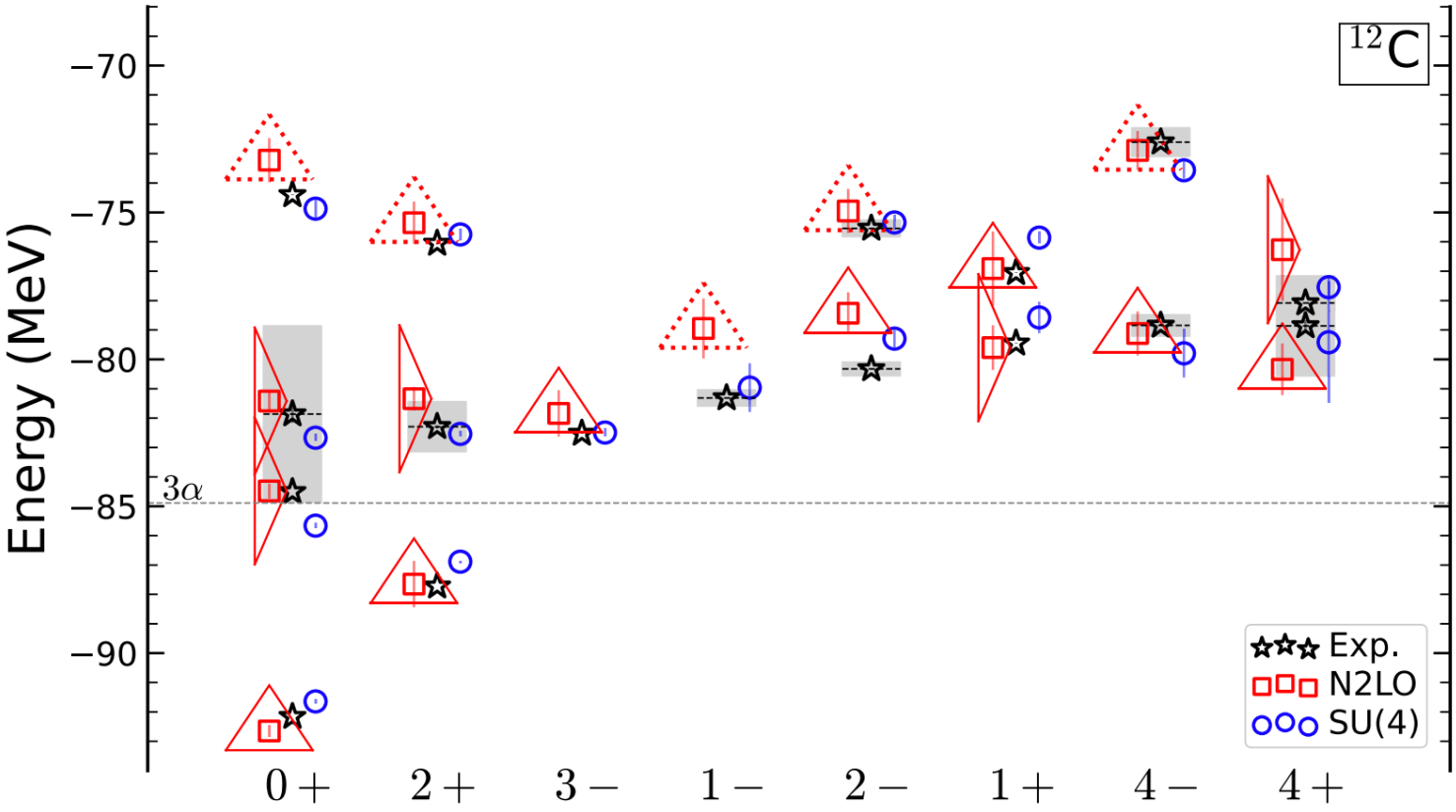

Shen, Elhatisari, Lähde, D.L., Lu, Meißner, Nature Commun. 14, 2777 (2023)

Wavefunction matching

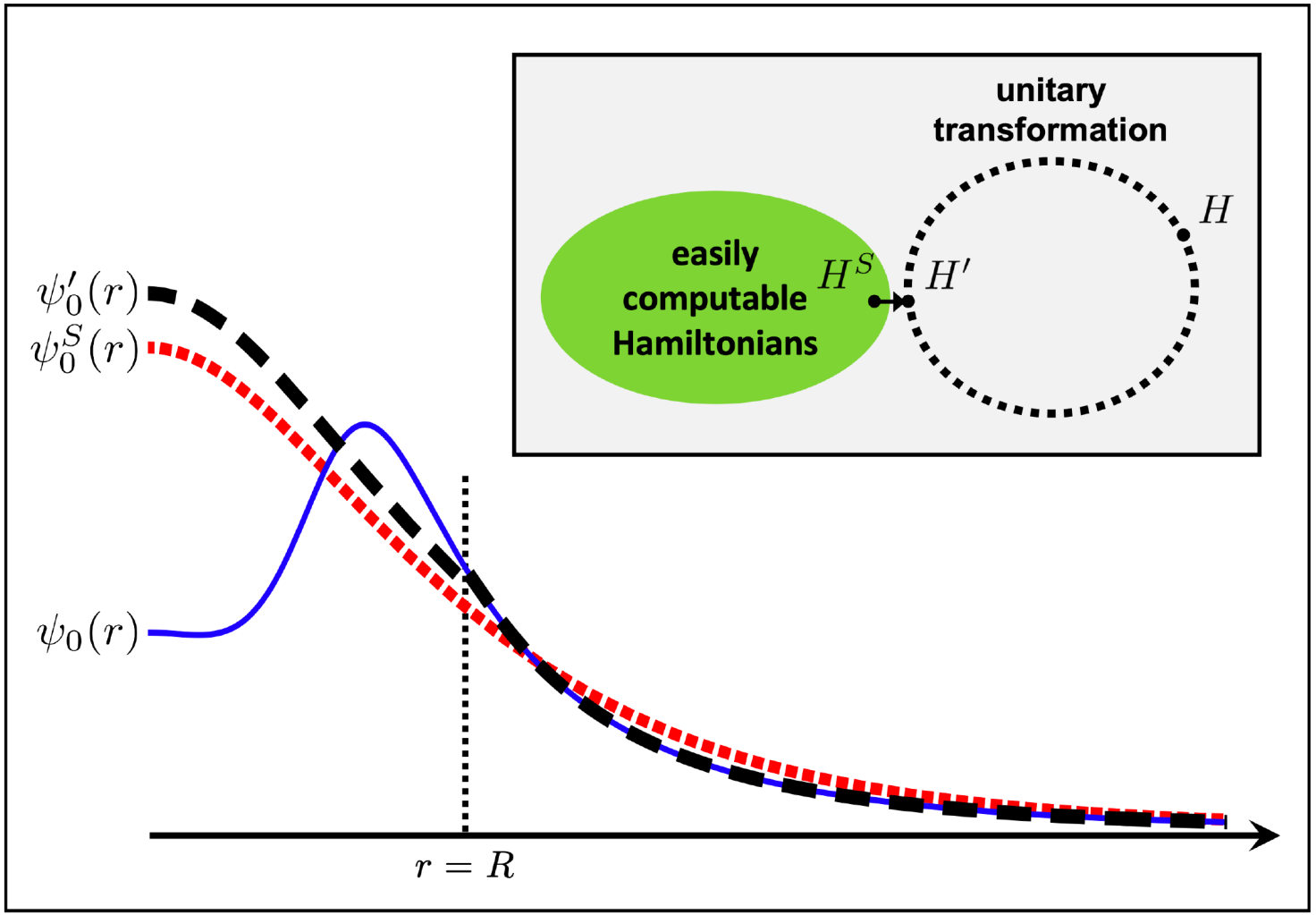

Elhatisari, Bovermann, Ma, Epelbaum, Frame, Hildenbrand, Krebs, Lähde, D.L., Li, Lu, M. Kim, Y. Kim, Meißner, Rupak, Shen, Song, Stellin, Nature 630, 59 (2024)

Ground state wavefunctions

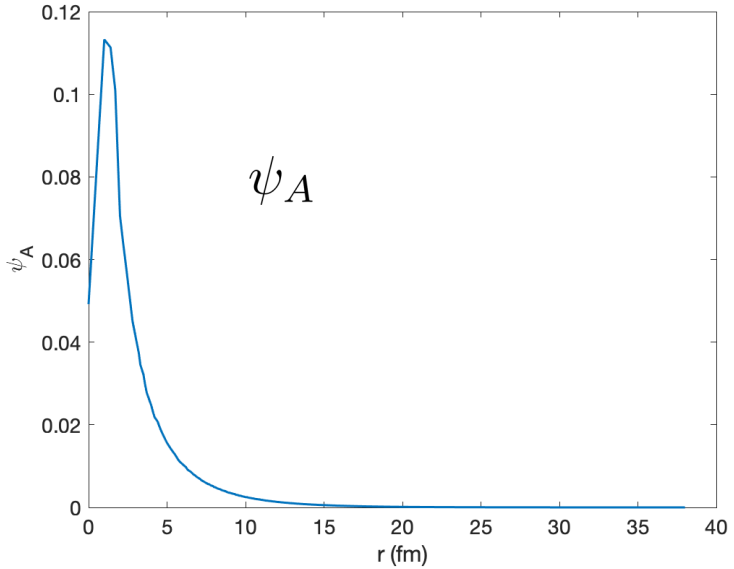

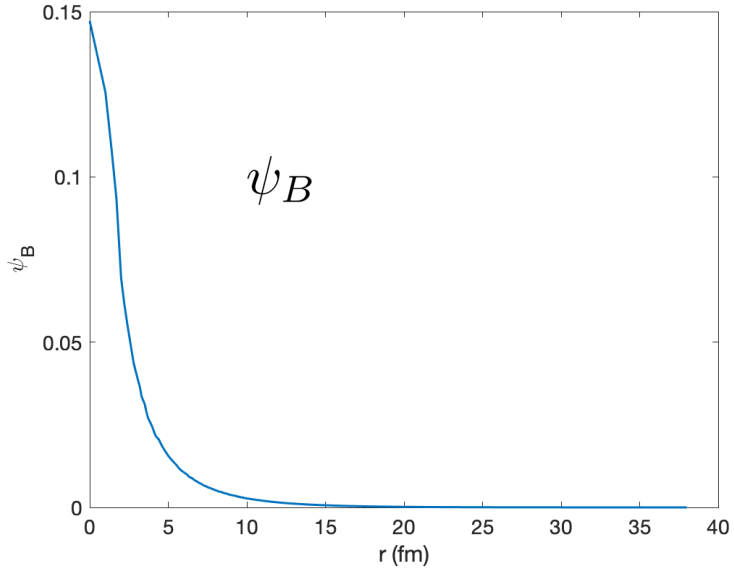

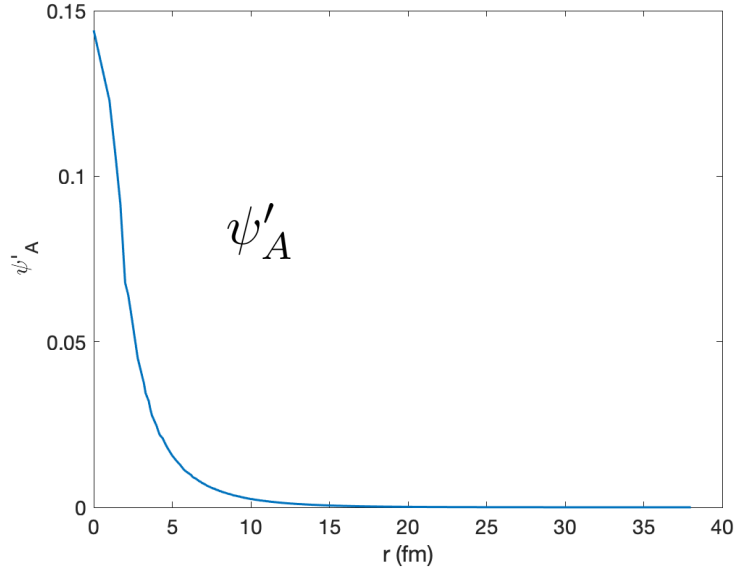

Try to compute the energies of H_A using the eigenfunctions of H_B and first-order perturbation theory. This doesn't work.

$E_{A,n} = E'_{A,n}$ (MeV)	$\langle \psi_{B,n} \vert H_A \vert \psi_{B,n} \rangle$ (MeV)
-1.2186	3.0088
0.2196	0.3289
0.8523	1.1275
1.8610	2.2528
3.2279	3.6991
4.9454	5.4786
7.0104	7.5996
9.4208	10.0674
12.1721	12.8799
15.2669	16.0458

Use wavefunction matching first to transform the Hamiltonian. Then the convergence of perturbation theory is much faster.

$E_{A,n} = E'_{A,n}$ (MeV)	$\langle\psi_{B,n}\|H_A\|\psi_{B,n}\rangle$ (MeV)	$\langle\psi_{B,n}\|H'_A\|\psi_{B,n}\rangle$ (MeV)
-1.2186	3.0088	-1.1597
0.2196	0.3289	0.2212
0.8523	1.1275	0.8577
1.8610	2.2528	1.8719
3.2279	3.6991	3.2477
4.9454	5.4786	4.9798
7.0104	7.5996	7.0680
9.4208	10.0674	9.5137
12.1721	12.8799	12.3163
15.2669	16.0458	15.4840

Binding energies

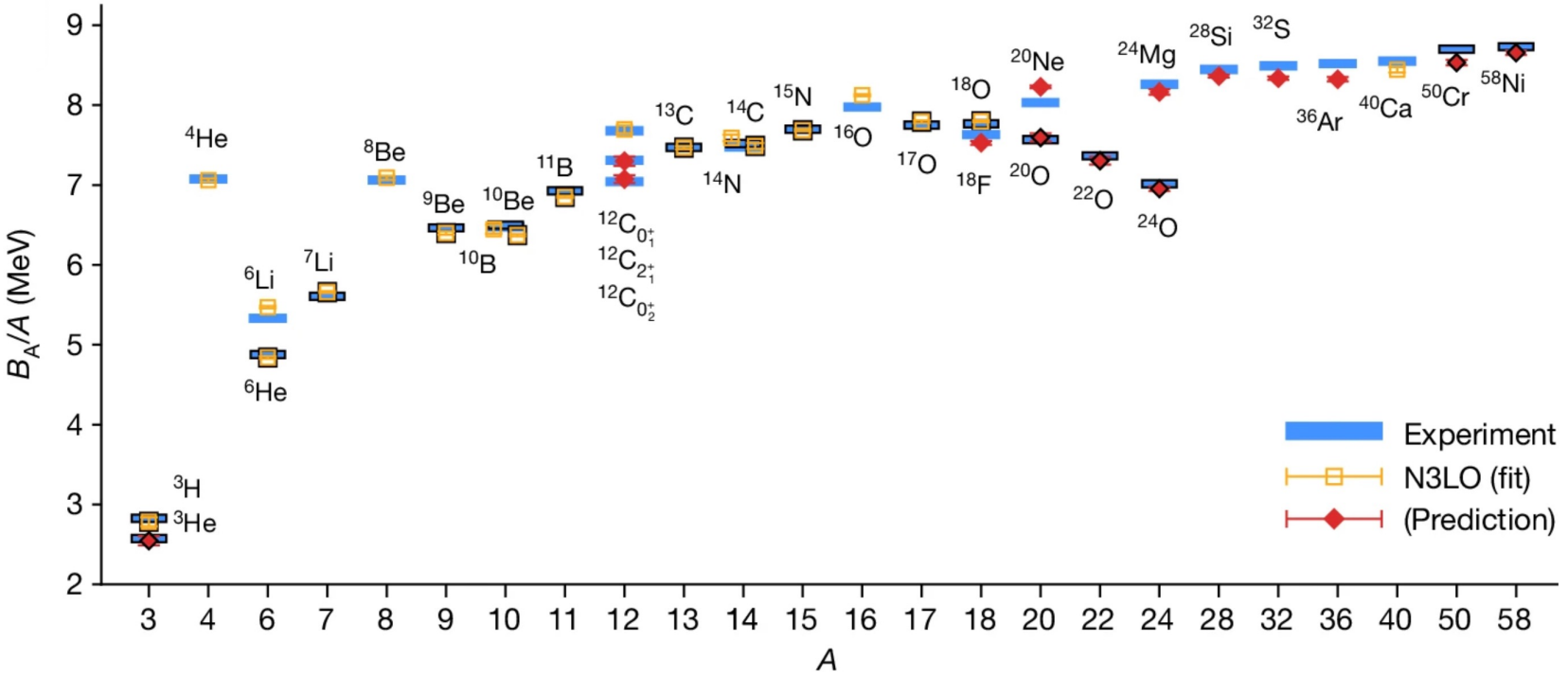

Elhatisari, Bovermann, Ma, Epelbaum, Frame, Hildenbrand, Krebs, Lähde, D.L., Li, Lu, M. Kim, Y. Kim, Meißner, Rupak, Shen, Song, Stellin, Nature 630, 59 (2024)

Charge radii

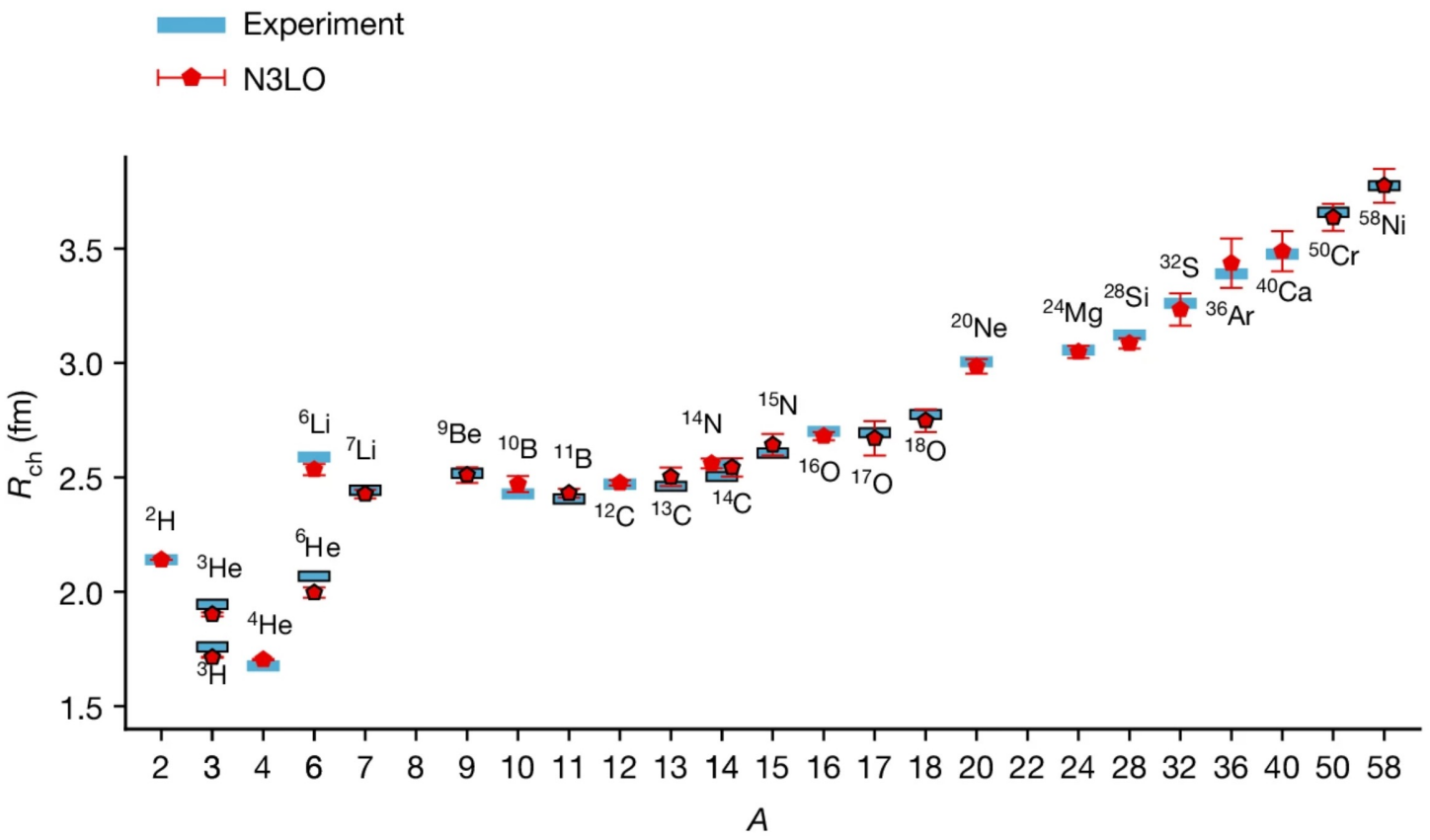

Elhatisari, Bovermann, Ma, Epelbaum, Frame, Hildenbrand, Krebs, Lähde, D.L., Li, Lu, M. Kim, Y. Kim, Meißner, Rupak, Shen, Song, Stellin, Nature 630, 59 (2024)

Neutron and nuclear matter

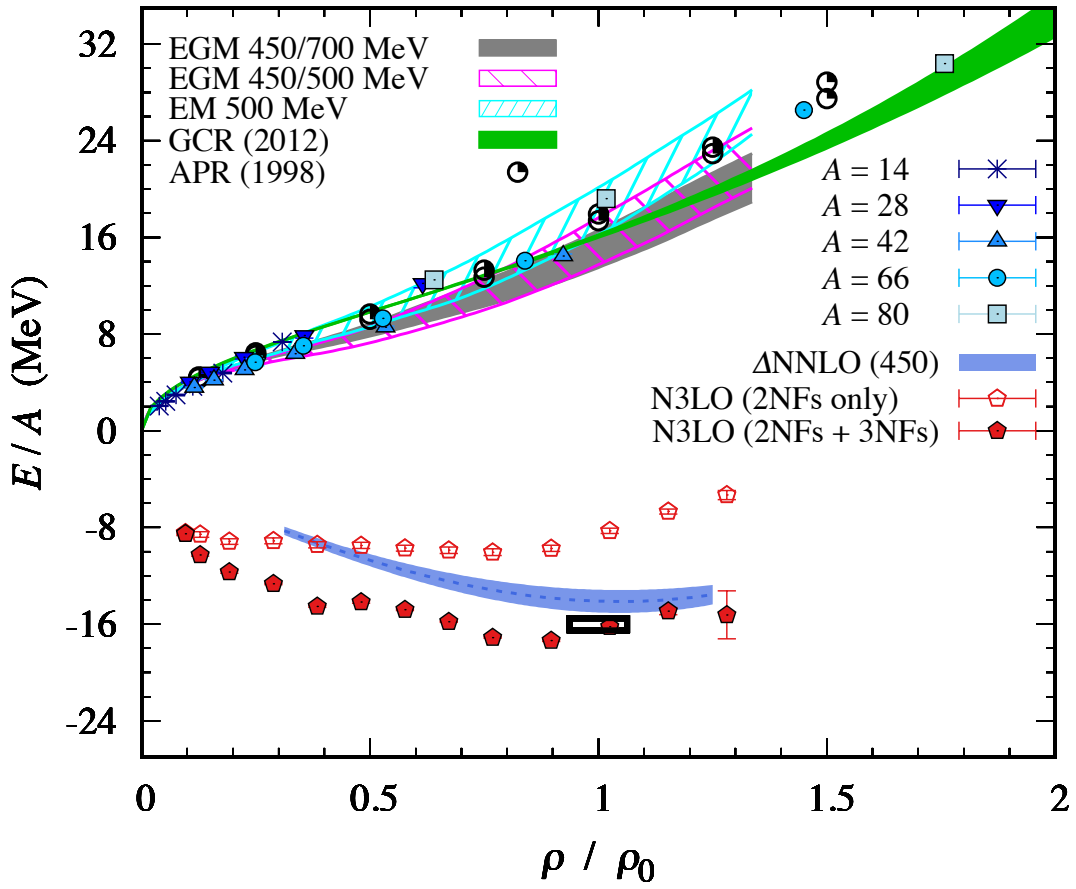

Figure adapted from Tews, Krüger, Hebeler, Schwenk, Phys. Rev. Lett. 110, 032504 (2013)

Elhatisari, Bovermann, Ma, Epelbaum, Frame, Hildenbrand, Krebs, Lähde, D.L., Li, Lu, M. Kim, Y. Kim, Meißner, Rupak, Shen, Song, Stellin, Nature 630, 59 (2024)

Charge radii of silicon isotopes

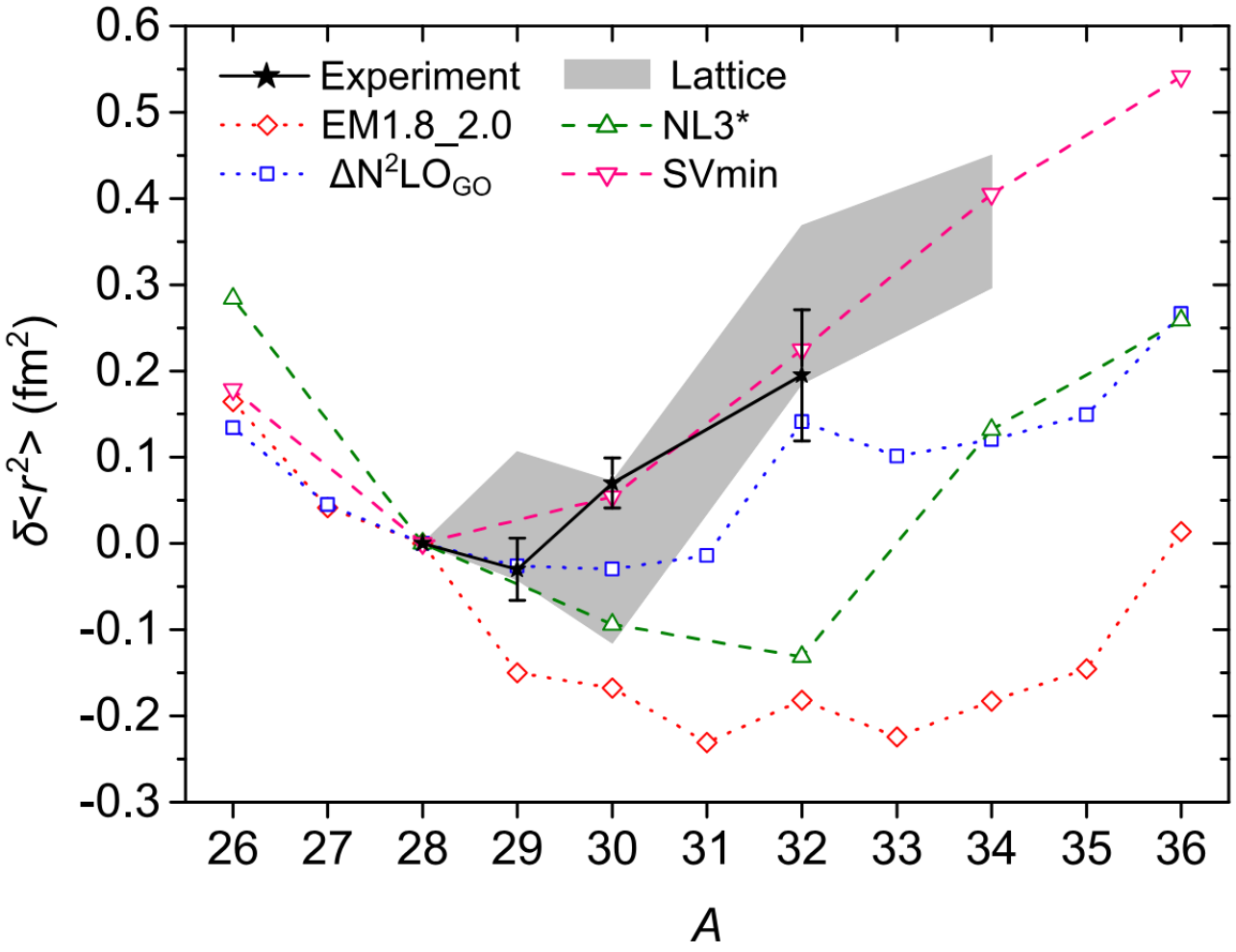

K. König et al., Phys. Rev. Lett. 132, 162502 (2024)

Structure of beryllium isotopes

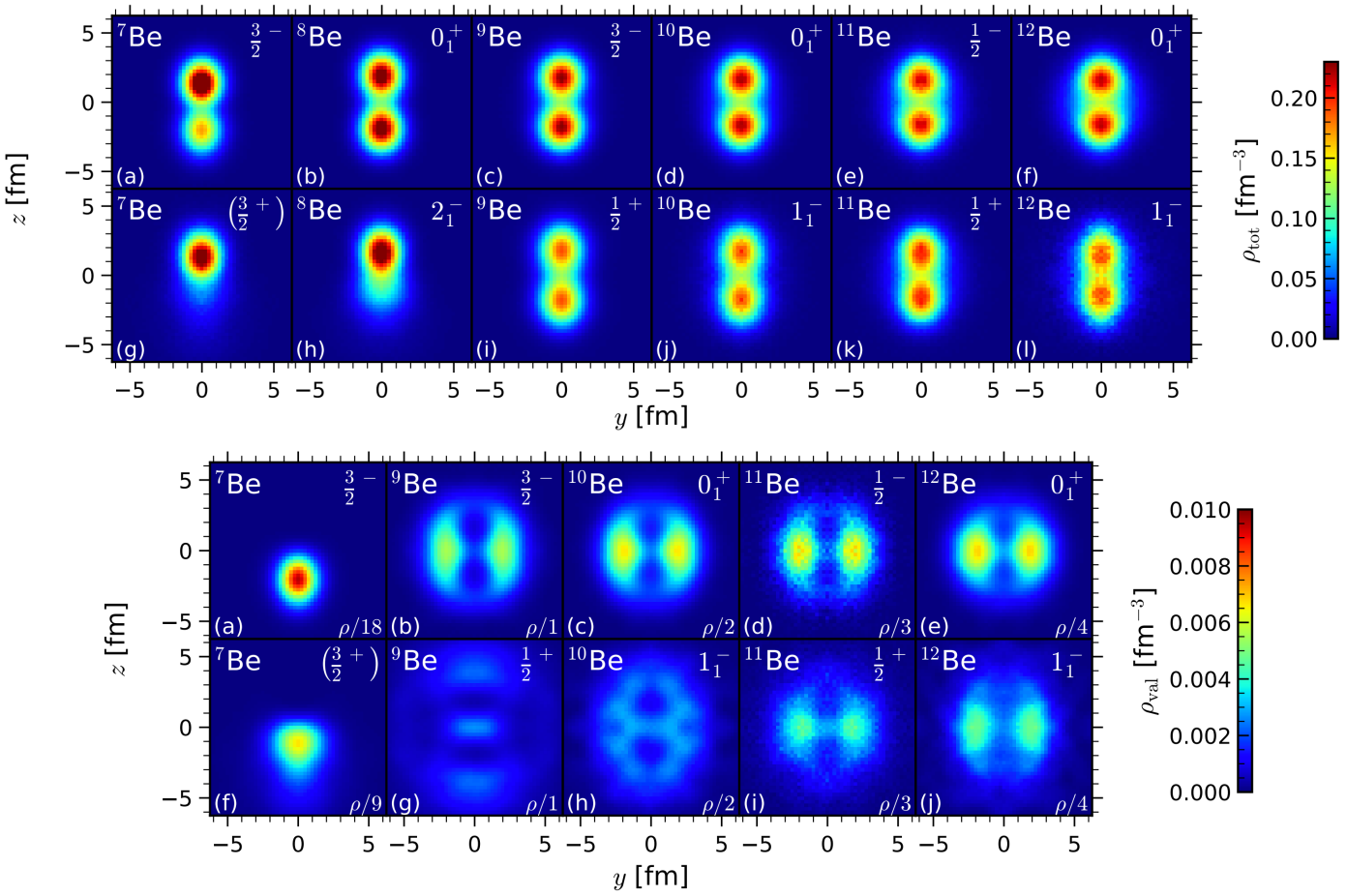

Shen, Elhatisari, D.L. Meißner, Ren, PRL 134, 162503 (2025)

Structure of beryllium isotopes

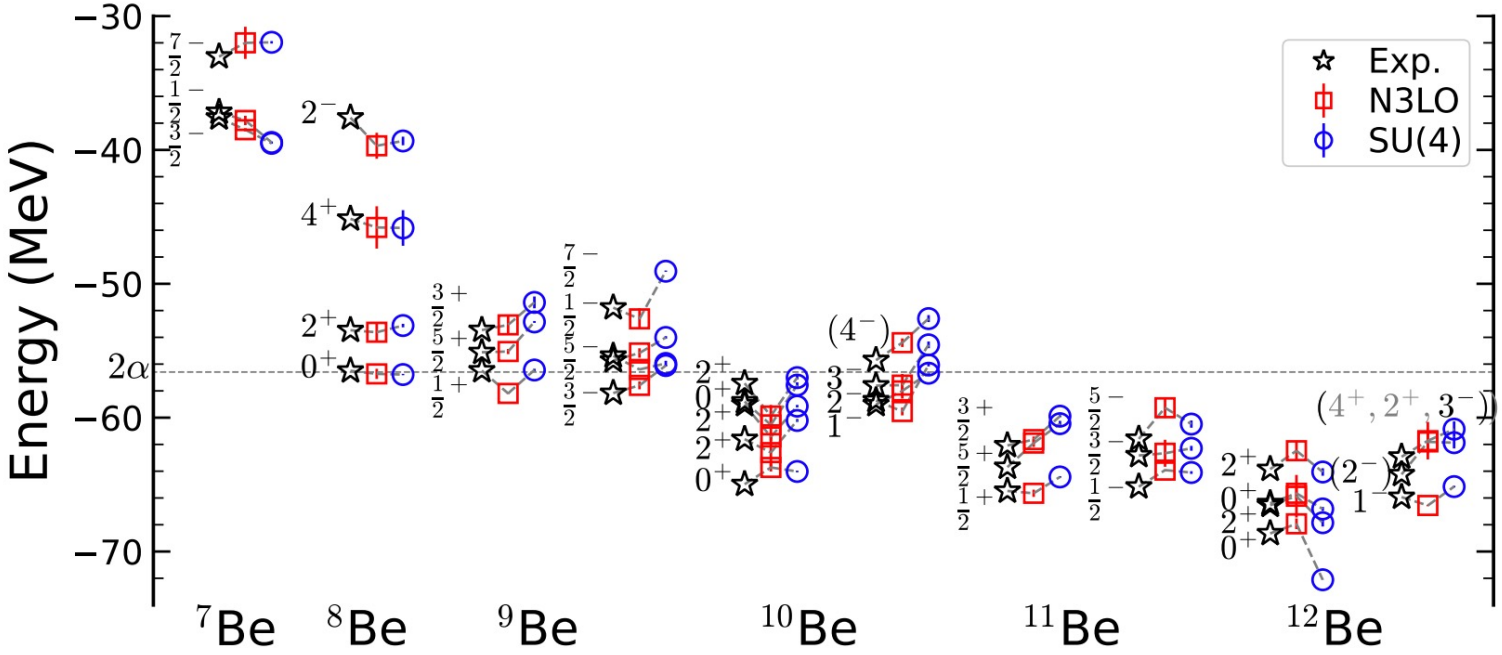

Shen, Elhatisari, D.L. Meißner, Ren, PRL 134, 162503 (2025)

arXiv:2602.17611

Evidence for Multimodal Superfluidity of Neutrons

Yuan-Zhuo Ma[1,2], Georgios Palkanoglou[3,4], Joseph Carlson[5], Stefano Gandolfi[5], Alexandros Gezerlis[4], Gabriel Given[1,2], Ashe Hicks[1,2], Dean Lee[1,2], Kevin E. Schmidt[6], and Jiabin Yu[7]

[1]Facility for Rare Isotope Beams, Michigan State University, East Lansing, Michigan 48824
[2]Department of Physics and Astronomy, Michigan State University, East Lansing, Michigan 48824
[3]TRIUMF, 4004 Wesbrook Mall, Vancouver, BC V6T 2A3, Canada
[4]Department of Physics, University of Guelph, Guelph, ON N1G 2W1, Canada
[5]Theoretical Division, Los Alamos National Laboratory, Los Alamos, NM 87545, USA
[6]Department of Physics, Arizona State University, Tempe, Arizona 85287, USA
[7]Department of Physics and Quantum Theory Project, University of Florida, Gainesville, FL 32611, USA

Superfluid condensation

BEC Theory

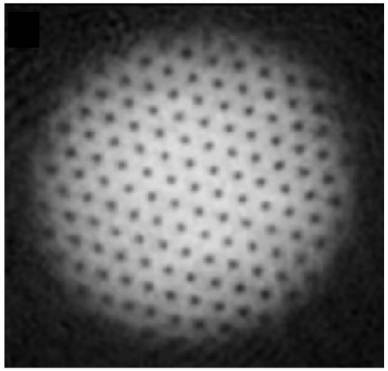

Ketterle, Zwierlein,
Ultracold Fermi Gases (2008)

BCS Theory

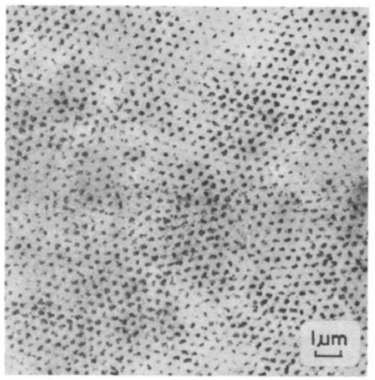

Essmann, Träuble,
Physics Letters A 27, 3 (1968)

Superfluid condensation

Bosonic superfluidity

$$\langle \Psi_0 | a^\dagger(\mathbf{r}) a(\mathbf{0}) | \Psi_0 \rangle$$

Fermionic superfluidity (S-wave)

$$\langle \Psi_0 | a^\dagger_\downarrow(\mathbf{r}) a^\dagger_\uparrow(\mathbf{r}) a_\uparrow(\mathbf{0}) a_\downarrow(\mathbf{0}) | \Psi_0 \rangle$$

Fermionic superfluidity (P-wave)

$$\langle \Psi_0 | a^\dagger_\uparrow(\mathbf{r}) a^\dagger_\uparrow(\mathbf{r}+\Delta\mathbf{r}) a_\uparrow(\Delta\mathbf{r}) a_\uparrow(\mathbf{0}) | \Psi_0 \rangle$$

We can also perform calculations in momentum space. But we need to compute cumulants to obtain irreducible contributions only.

Yang, RMP **34**, 694 (1962)

Multimodal superfluidity

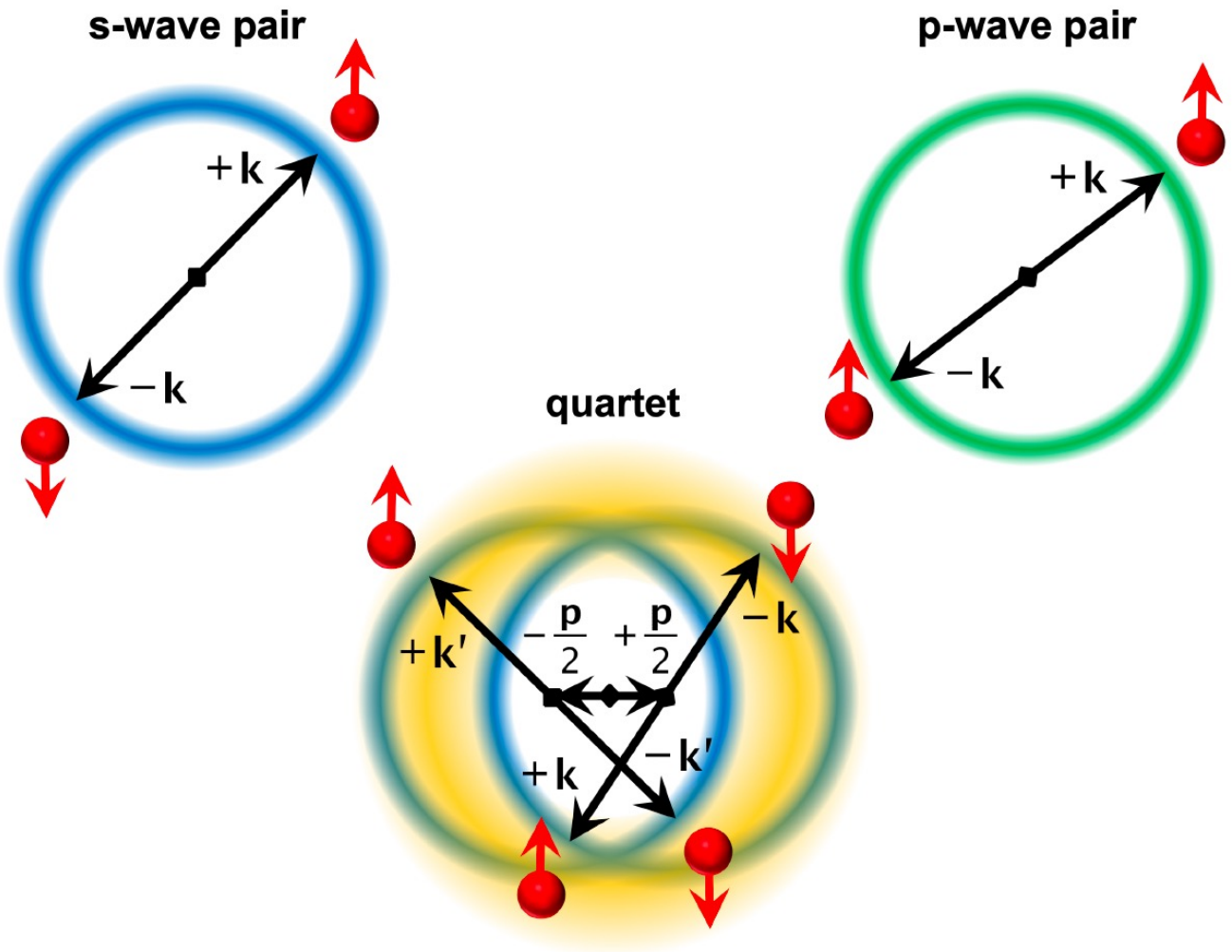

Quantum phase diagram

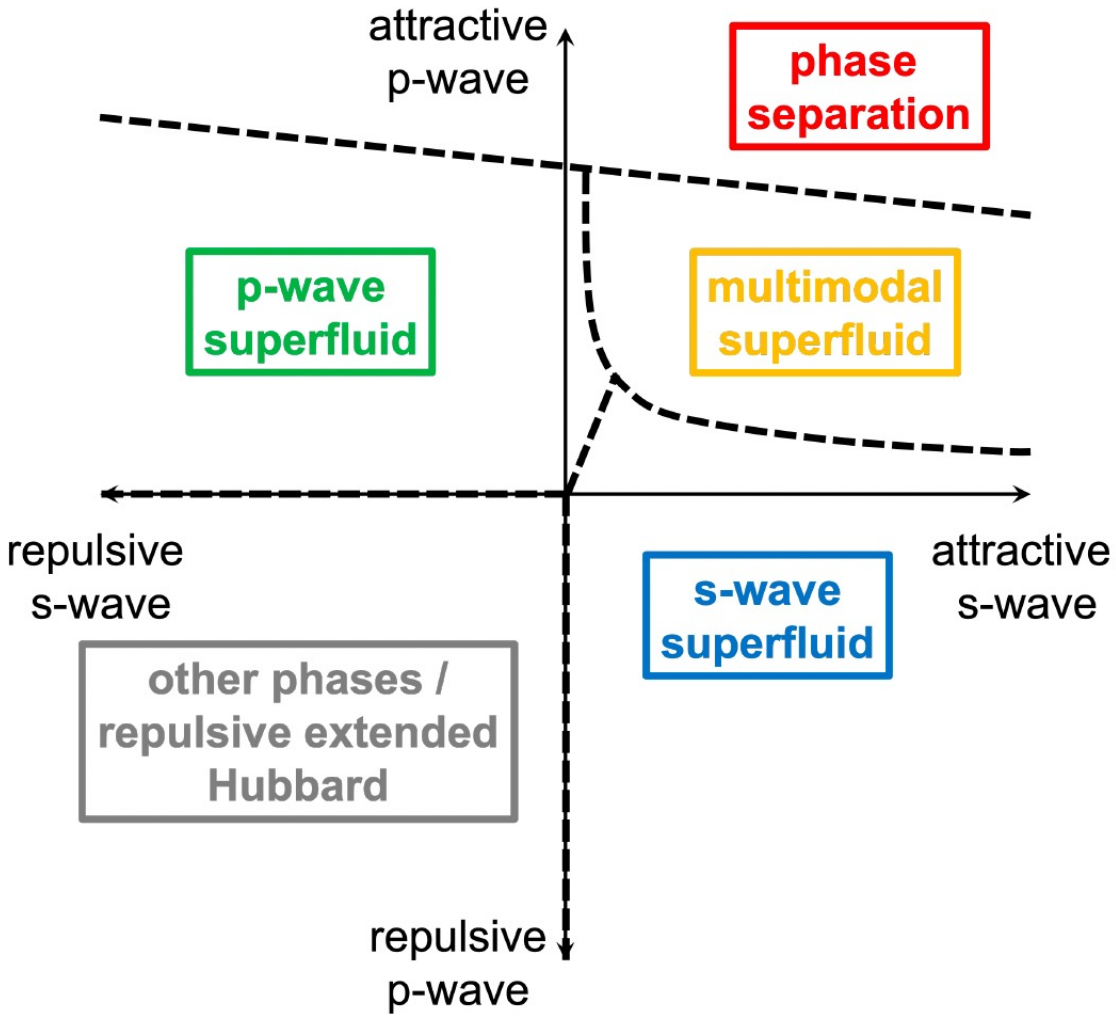

Neutron matter with N3LO interactions

$$k_F = 167 \text{ MeV}$$

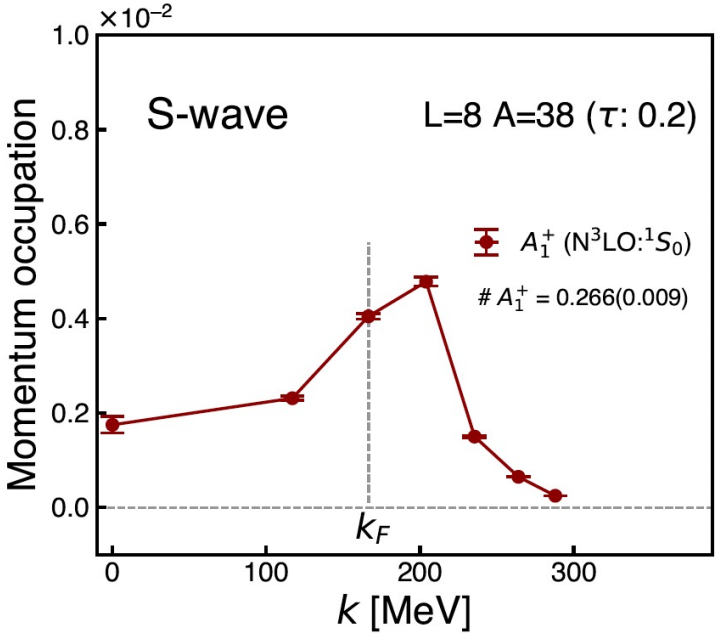

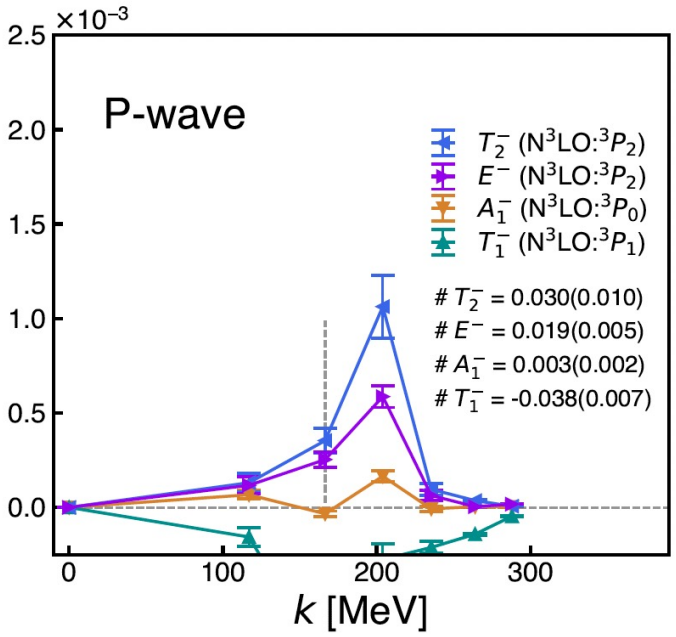

Neutron matter with N3LO interactions

$$k_F = 167 \text{ MeV}$$

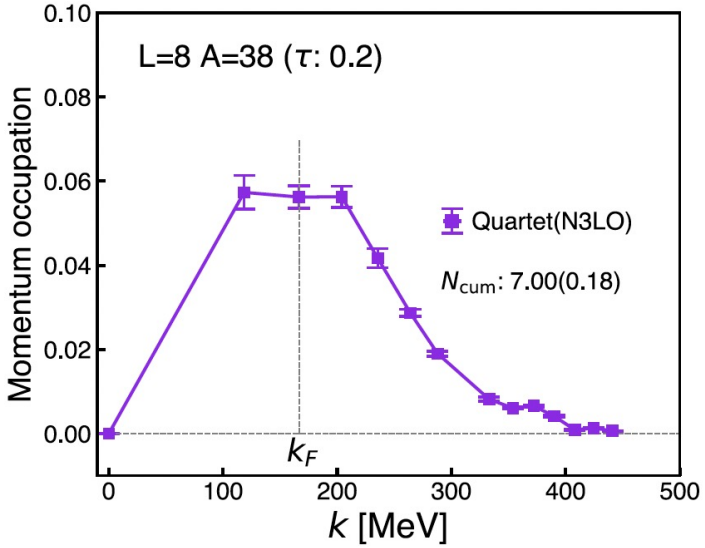

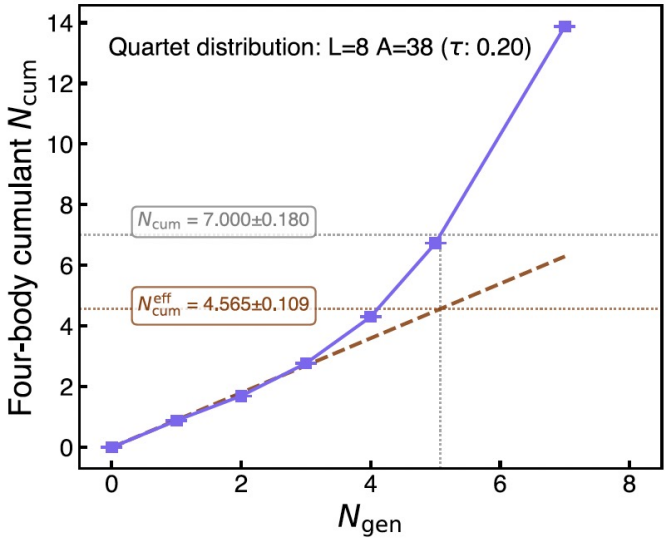

s-wave pairs	1.40(5)%
p-wave pairs	$^3P_0 = 0.02(1)\%$, $^3P_2 = 0.26(8)\%$
quartets	48(1)%

Neutron matter with N3LO interactions

$$k_F = 269 \text{ MeV}$$

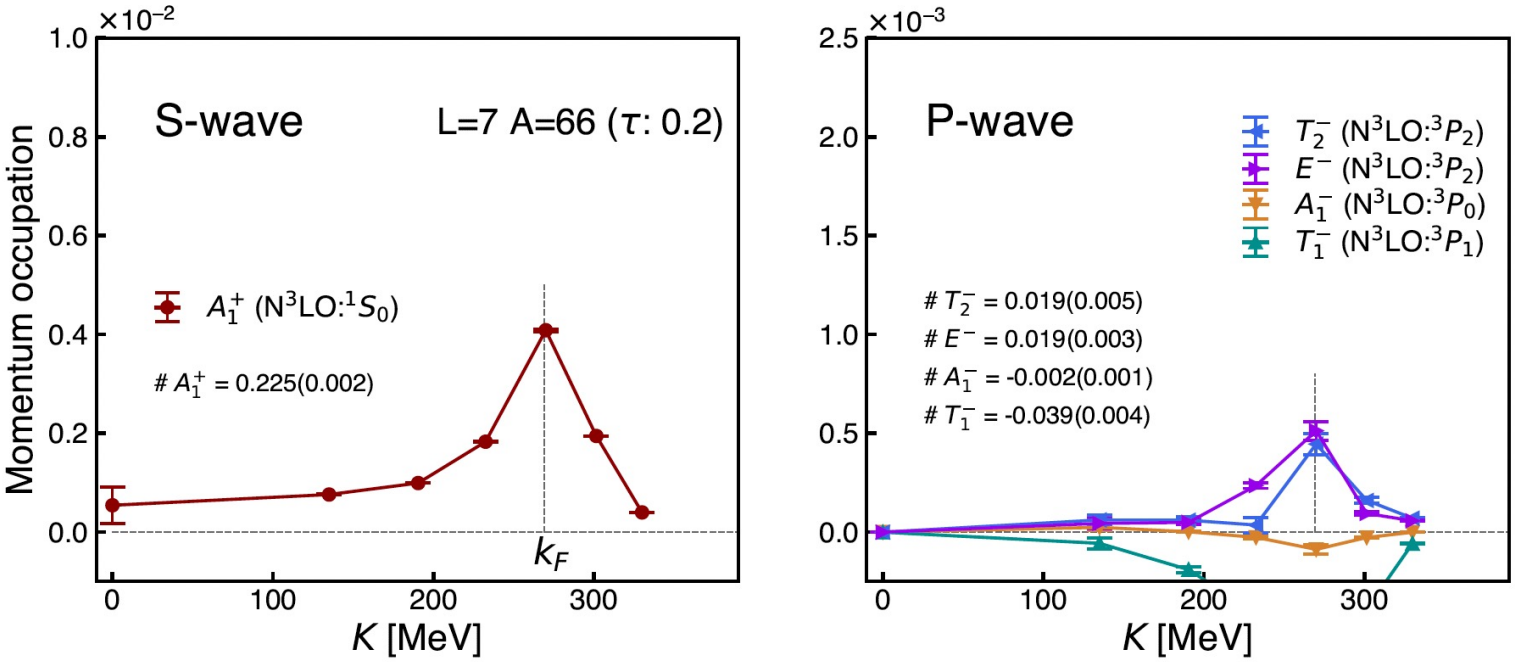

Neutron matter with N3LO interactions

$$k_F = 269 \text{ MeV}$$

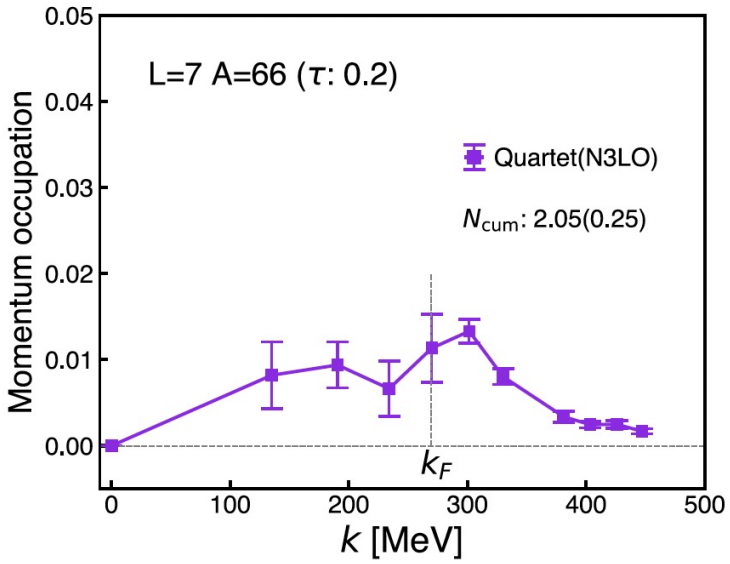

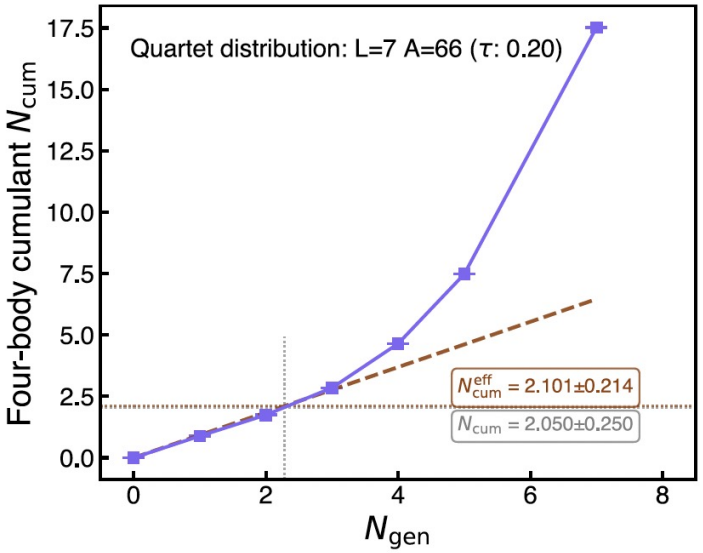

s-wave pairs	$0.68(1)\%$
p-wave pairs	${}^3P_0 = 0.00\%$, ${}^3P_2 = 0.12(2)\%$
quartets	$13(1)\%$

Experimental evidence

S-wave pair binding in MeV

Nuclei	Predominant Orbitals	$2\Delta_S$
$S_n\{^{17}_{8}\mathrm{O}_9, ^{18}_{8}\mathrm{O}_{10}\}_+$	$(1d_{5/2})^2$	3.902
$\frac{1}{2}S_n\{^{17}_{8}\mathrm{O}_9, ^{18}_{8}\mathrm{O}_{10}, ^{19}_{8}\mathrm{O}_{11}\}_-$	$(1d_{5/2})^2$	3.996(1)
$\frac{1}{4}S_n\{^{17}_{8}\mathrm{O}_9, ^{18}_{8}\mathrm{O}_{10}, ^{19}_{8}\mathrm{O}_{11}, ^{20}_{8}\mathrm{O}_{12}\}_+$	$(1d_{5/2})^2$	3.934(2)
$S_n\{^{41}_{20}\mathrm{Ca}_{21}, ^{42}_{20}\mathrm{Ca}_{22}\}_+$	$(1f_{7/2})^2$	3.118
$\frac{1}{2}S_n\{^{41}_{20}\mathrm{Ca}_{21}, ^{42}_{20}\mathrm{Ca}_{22}, ^{43}_{20}\mathrm{Ca}_{23}\}_-$	$(1f_{7/2})^2$	3.333
$\frac{1}{2}S_n\{^{41}_{20}\mathrm{Ca}_{21}, ^{42}_{20}\mathrm{Ca}_{22}, ^{43}_{20}\mathrm{Ca}_{23}, ^{44}_{20}\mathrm{Ca}_{24}\}_-$	$(1f_{7/2})^2$	3.353
$S_n\{^{209}_{82}\mathrm{Pb}_{127}, ^{210}_{82}\mathrm{Pb}_{128}\}_+$	$(2g_{9/2})^2$	1.248(2)
$\frac{1}{2}S_n\{^{209}_{82}\mathrm{Pb}_{127}, ^{210}_{82}\mathrm{Pb}_{128}, ^{211}_{82}\mathrm{Pb}_{129}\}_-$	$(2g_{9/2})^2$	1.299(2)
$\frac{1}{4}S_n\{^{209}_{82}\mathrm{Pb}_{127}, ^{210}_{82}\mathrm{Pb}_{128}, ^{211}_{82}\mathrm{Pb}_{129}, ^{212}_{82}\mathrm{Pb}_{130}\}_+$	$(2g_{9/2})^2$	1.309(2)

Experimental evidence

P-wave pair binding in MeV

Nuclei	Predominant Orbitals	$2\Delta_P$
$S_n\{^{17}_{8}\mathrm{O}_9(\frac{3}{2}^+), ^{18}_{8}\mathrm{O}_{10}(1^+)\}_+$	$1d_{5/2} \otimes 1d_{3/2}$	0.172(12)
$\frac{1}{2}S_n\{^{55}_{26}\mathrm{Fe}_{29}(\frac{5}{2}^-), ^{56}_{26}\mathrm{Fe}_{30}(1^+), ^{57}_{26}\mathrm{Fe}_{31}(\frac{5}{2}^-)\}_-$	$2p_{3/2} \otimes 1f_{5/2}$	0.139(3)
$\frac{1}{2}S_n\{^{57}_{28}\mathrm{Ni}_{29}(\frac{5}{2}^-), ^{58}_{28}\mathrm{Ni}_{30}(1^+), ^{59}_{28}\mathrm{Ni}_{31}(\frac{5}{2}^-)\}_-$	$2p_{3/2} \otimes 1f_{5/2}$	0.245(1)

Experimental evidence

Quartet binding in MeV

Nuclei	Predominant Orbitals	$4\Delta_Q$
$S_{2n}\{^{6}_{2}\mathrm{He}_4, ^{8}_{2}\mathrm{He}_4\}_+$	$(1p_{3/2})^4$	1.150
$\frac{1}{2}S_{2n}\{^{18}_{8}\mathrm{O}_{10}, ^{20}_{8}\mathrm{O}_{12}, ^{22}_{8}\mathrm{O}_{14}\}_-$	$(1d_{5/2})^4$	0.142(28)
$\frac{1}{2}S_{2n}\{^{42}_{20}\mathrm{Ca}_{22}, ^{44}_{20}\mathrm{Ca}_{24}, ^{46}_{20}\mathrm{Ca}_{26}\}_-$	$(1f_{7/2})^4$	0.236(1)
$\frac{1}{2}S_{2n}\{^{44}_{20}\mathrm{Ca}_{24}, ^{46}_{20}\mathrm{Ca}_{26}, ^{48}_{20}\mathrm{Ca}_{28}\}_+$	$(1f_{7/2})^4$	0.332(3)
$\frac{1}{2}S_{2n}\{^{106}_{50}\mathrm{Sn}_{56}, ^{108}_{50}\mathrm{Sn}_{58}, ^{110}_{50}\mathrm{Sn}_{60}\}_+$	combination	0.033(11)
$\frac{1}{2}S_{2n}\{^{108}_{50}\mathrm{Sn}_{58}, ^{110}_{50}\mathrm{Sn}_{60}, ^{112}_{50}\mathrm{Sn}_{62}\}_-$	combination	0.007(17)
$\frac{1}{2}S_{2n}\{^{110}_{50}\mathrm{Sn}_{60}, ^{112}_{50}\mathrm{Sn}_{62}, ^{114}_{50}\mathrm{Sn}_{64}\}_+$	combination	0.025(16)
$\frac{1}{2}S_{2n}\{^{112}_{50}\mathrm{Sn}_{62}, ^{114}_{50}\mathrm{Sn}_{64}, ^{116}_{50}\mathrm{Sn}_{66}\}_-$	combination	0.015(7)
$\frac{1}{2}S_{2n}\{^{114}_{50}\mathrm{Sn}_{64}, ^{116}_{50}\mathrm{Sn}_{66}, ^{118}_{50}\mathrm{Sn}_{68}\}_+$	combination	0.050(30)
$\frac{1}{2}S_{2n}\{^{194}_{82}\mathrm{Pb}_{112}, ^{196}_{82}\mathrm{Pb}_{114}, ^{198}_{82}\mathrm{Pb}_{116}\}_+$	combination	0.047(22)
$\frac{1}{2}S_{2n}\{^{196}_{82}\mathrm{Pb}_{114}, ^{198}_{82}\mathrm{Pb}_{116}, ^{200}_{82}\mathrm{Pb}_{118}\}_-$	combination	0.057(16)
$\frac{1}{2}S_{2n}\{^{198}_{82}\mathrm{Pb}_{116}, ^{200}_{82}\mathrm{Pb}_{118}, ^{202}_{82}\mathrm{Pb}_{120}\}_+$	combination	0.021(15)
$\frac{1}{2}S_{2n}\{^{200}_{82}\mathrm{Pb}_{118}, ^{202}_{82}\mathrm{Pb}_{120}, ^{204}_{82}\mathrm{Pb}_{122}\}_-$	combination	0.013(13)
$\frac{1}{2}S_{2n}\{^{202}_{82}\mathrm{Pb}_{120}, ^{204}_{82}\mathrm{Pb}_{122}, ^{206}_{82}\mathrm{Pb}_{124}\}_+$	combination	0.014(7)
$\frac{1}{2}S_{2n}\{^{204}_{82}\mathrm{Pb}_{122}, ^{206}_{82}\mathrm{Pb}_{124}, ^{208}_{82}\mathrm{Pb}_{126}\}_-$	combination	0.110(2)
$\frac{1}{2}S_{2n}\{^{210}_{82}\mathrm{Pb}_{128}, ^{212}_{82}\mathrm{Pb}_{130}, ^{214}_{82}\mathrm{Pb}_{132}\}_-$	$(2g_{9/2})^4$	0.014(2)
$\frac{1}{2}S_{2n}\{^{212}_{84}\mathrm{Po}_{128}, ^{214}_{84}\mathrm{Po}_{130}, ^{216}_{84}\mathrm{Po}_{132}\}_-$	$(2g_{9/2})^4$	0.019(1)
$\frac{1}{2}S_{2n}\{^{214}_{84}\mathrm{Po}_{130}, ^{216}_{84}\mathrm{Po}_{132}, ^{218}_{84}\mathrm{Po}_{134}\}_+$	$(2g_{9/2})^4$	0.015(2)
$\frac{1}{2}S_{2n}\{^{214}_{86}\mathrm{Rn}_{128}, ^{216}_{86}\mathrm{Rn}_{130}, ^{218}_{86}\mathrm{Rn}_{132}\}_-$	$(2g_{9/2})^4$	0.079(12)

Summary

We have reviewed nuclear lattice effective field theory and recent algorithmic advances such as the pinhole algorithm and wavefunction matching. We presented calculations of nuclear structure demonstrating clustering in carbon-12, neon-20, and the beryllium isotopes as well as the charge radii of the silicon isotopes. Nuclear lattice simulations are useful for providing initial states for relativistic ion collisions and can be similarly useful for future EIC experiments. We have also reported theoretical and experimental evidence for multimodal superfluidity in neutron-rich matter.